2005

A New Approach to the Synthesis of PVC Graft Copolymers

Guangde Chen
College of William & Mary - Arts & Sciences

A NEW APPROACH TO THE SYNTHESIS OF PVC GRAFT COPOLYMERS

A Thesis

Presented to

The Faculty of the Department of Chemistry

The College of William and Mary in Virginia

In Partial Fulfillment

Of the Requirements for the Degree of

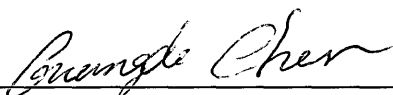Master of Science

By

Guangde Chen

2005

ii

TABLE OF CONTENTS

ACKNOWLEDGEMENTS

LIST OF TABLES

LIST OF FIGURES

viii

ABSTRACT

A new approach to the synthesis of poly(vinyl chloride) (PVC) graft copolymers is described. It involves the abstraction of chlorine atoms from PVC by the tributyltin free radical in the presence of monomers that can polymerize by a free-radical route. Rate constants for chlorine abstraction relative to those for addition of $Bu_3Sn\cdot$ to vinyl acetate (VAc) or isobutylene (Ib) were determined by using 2-chlorobutane as a PVC model compound. The values obtained revealed that Ib was the less reactive monomer and that the addition of $Bu_3Sn\cdot$ to alkene linkages is retarded strongly by electron-donating groups. A PVC-g-PVAc copolymer was prepared from PVC and VAc by using hexa-n-butylditin as a photoinitiator and then removing the byproduct PVAc by selective extraction with methanol. The PVC-g-PVAc was analyzed by GPC, FTIR, ^1H and ^{13}C NMR, TGA, and DSC. Results obtained showed that this copolymer had a molecular weight which was significantly greater than that of the original PVC, as well as a monomodal molecular-weight distribution. The copolymer also was demonstrated to contain both VC and VAc monomer units. Moreover, its thermal stability was somewhat less than that of the starting PVC, and it exhibited a single glass-transition temperature that fell between those of PVC and PVAc. A material identified tentatively as PVC-g-PIb was prepared in a similar way from PVC and Ib and characterized by GPC, TGA, and DSC measurements.

A NEW APPROACH TO THE SYNTHESIS OF

PVC GRAFT COPOLYMERS

I. Introduction

The chemical combination of two or more incompatible polymers into sequential copolymers, i.e., block and graft copolymers, often leads to a unique combination of physical properties not originally present in either of the two component polymers or in their physical blends. For example, the chemical combination of rubbery and glassy polymers may lead to "thermoplastic elastomer" materials that exhibit elastomeric behavior in the absence of chemical cross-links.[1]

Poly(vinyl chloride) (PVC) has been one of the most widely used vinyl polymers in the world for more than 70 years. However, some of the public discussion on the supposed environmental dangers and hazards of chlorine chemistry has attempted to weaken the importance of PVC on our daily life. This problem has aroused the attention of scientists and has been responsible, in part, for their efforts to modify the properties of PVC. Fortunately, owing to the presence of halogen atoms as reactive sites for branching, PVC is a good starting material for the synthesis of graft copolymers.[2]

Graft copolymers derived from PVC are new materials whose physical properties may be improved considerably over those of PVC itself. Since the 1960s, anionic, cationic, and free-radical graft copolymerizations of PVC have been studied.

A. Anionic graft copolymers from PVC

Anionic graft copolymers of PVC can generally be obtained from nucleophilic substitution reactions of chlorine atoms (Figure 1). As a result, a polymeric anion is

grafted onto the PVC backbone. Appropriate displacement agents are characterized by a strongly nucleophilic character, while their basicity should be low in order to avoid base-promoted dehydrochlorination. Also, to avoid undesired termination of activity, air and polar species such as moisture must be excluded. Therefore, this kind of approach has some limitations. So, as a result, few copolymers of PVC have been prepared by this process.

$$\text{---}(\text{CH}_2\text{---}\underset{\underset{\text{Cl}}{|}}{\text{CH}})\text{---} \quad + \quad M^{\ominus} \longrightarrow \text{---}(\text{CH}_2\text{---}\underset{\underset{\text{M}}{|}}{\text{CH}})\text{---} \quad + \quad \text{Cl}^{\ominus}$$

PVC repeating unit   Macrocarbanion   PVC copolymer
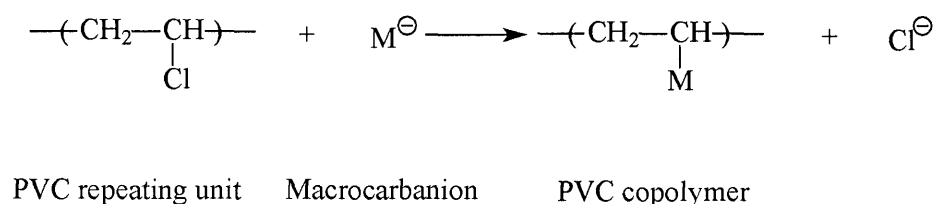
Figure 1. Anionic graft copolymer from PVC

The functionalization[3] of PVC also is an objective pursued by scientists via nucleophilic substitution reactions of chlorine atoms. If such a modification reaction is performed with a selective bifunctional molecule such that only one functionality reacts with the PVC, while the other reacts with another polymer, then the resulting copolymer will be provided with new physical properties. Furthermore, if PVC is modified with a nucleophilic reagent that also contains a basic nitrogen atom, such as 4-mercaptopyridine or 4-mercapto-N,N-dimethylaniline,[4] then the resultant PVCs with pendant tertiary amino groups can easily be transformed into ionomers. These products have potential applications as ion exchange resins which act as dynamic cars that drive the PVC chains between the inorganic layers of materials such as montmorillonite clay. As a result, the PVC bonds with the inorganic aluminosilicate layers and tends to form a nanocomposite whose thermal stability is enhanced.

B. Cationic graft copolymers from PVC

Cationic grafting (Figure 2) involves the formation of a carbocation on the polymer backbone via abstraction of a chloride anion by a Lewis acid. Initiation of graft copolymerization then takes place from the polymeric cation.
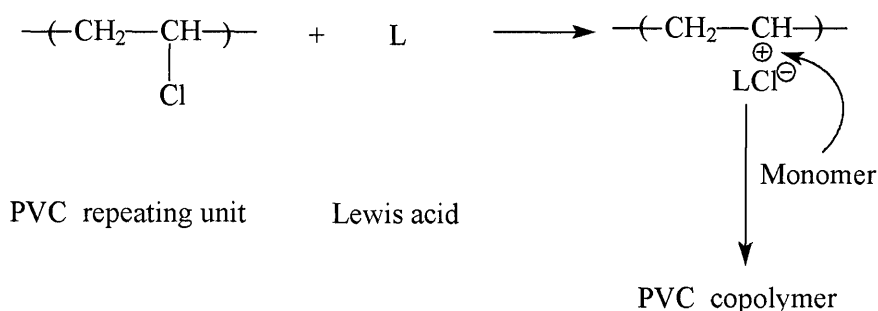
Figure 2. Cationic graft copolymer from PVC

1. Cationic catalysts

These catalysts principally include the trialkylaluminums and dialkylaluminum monohalides.[5] In general, for the synthesis of PVC grafts, techniques using alkylaluminums (such as Et_3Al) are far superior to earlier methods employing conventional Friedel-Crafts halides (such as Et_2AlCl), because the former processes are more readily controllable, so that gelation and degradation can thus be easily minimized or avoided. Hence the products are cleaner and consequently easier to analyze.

2. Monomers

Because of the electrophilic reactivity of polymeric cations, monomers containing election-withdrawing groups cannot be used, owing to their failure to polymerize

cationically. Thame et al.[6] have succeeded in grafting butadiene and isobutylene onto PVC by using cationic chain transfer.

3. Backbone cation sites

These cations form mainly at "labile-halogen" sites such as allylic and tertiary chloride. In this case, it is better to increase the number of these labile sites by a prior dehydrochlorination of PVC or by the use of a copolymer of vinyl chloride with a monomer such as 2-chloropropene. However, these processes increase production costs and also introduce structural defects which, if not removed completely by graft formation, will decrease the thermal stability.

C. Free-radical graft copolymers from PVC

For the free-radical graft copolymerization process, it was thought that grafting occurred by the transfer of growing or primary radicals to the main chain of PVC via (a) an abstraction of a chlorine or tertiary hydrogen atom and (b) subsequent initiation from the resultant PVC radicals (Figure 3).[7]

The free-radical grafting onto PVC is applicable to a larger number of monomers than are the anionic and cationic methods. However, the resulting graft copolymers are always contaminated by a significant amount of free homopolymer; whereas both anionic (by grafting onto)[8] and cationic (by grafting from)[9] methods afford well-defined graft copolymers. This problem occurs because many types of initiator radicals will add competitively to the monomer which is to be grafted, thereby initiating its homopolymerization during the free-radical grafting process.

$$—(\!-CH_2—\underset{\underset{Cl}{|}}{CH}\!-)— \quad + \quad R\bullet \quad \longrightarrow \quad —(\!-CH_2—\underset{\underset{\bullet}{|}}{CCl}\!-)— \quad + \quad RH$$

PVC repeating unit

Monomer
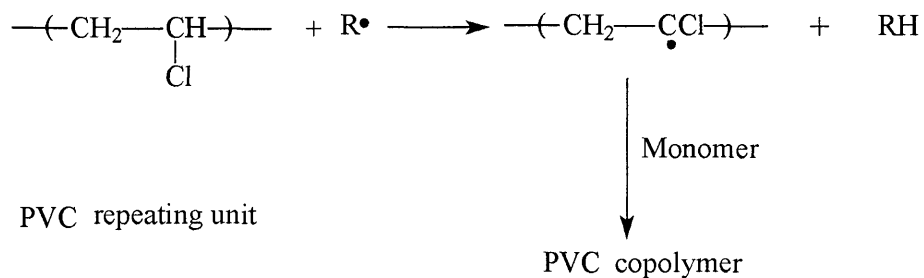
PVC copolymer

Figure 3. Free-radical graft copolymer from PVC

Another disadvantage of the conventional radical graft copolymerization lies in the special structure of PVC.

If a chloromethylene hydrogen is abstracted, the branch point resulting from grafting with any monomer will incorporate tertiary chloride and thus be thermally labile, as indicated in Figure 4.

$$—CH_2\underset{\underset{H}{|}}{\overset{\overset{Cl}{|}}{C}}CH_2— \quad + \quad R\bullet \quad \longrightarrow \quad —CH_2\underset{\underset{\bullet}{|}}{\overset{\overset{Cl}{|}}{C}}CH_2— \quad + \quad RCl$$

M_1(Monomer)

$$—CH_2\overset{\overset{Cl}{|}}{\underset{\underset{(M_1)_{\overline{n}}}{|}}{C}}CH_2—$$

Chloromethylene hydrogen

Tertiary chloride (labile structure)
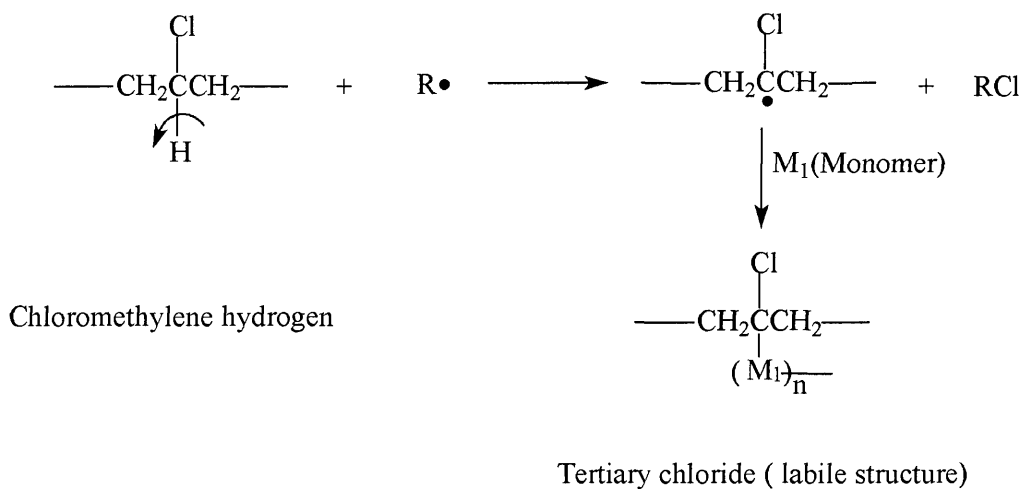
Figure 4. Labile structure from chloromethylene hydrogen removal

Moreover, if a methylene hydrogen is abstracted, the resultant carbon-centered radical, instead of adding to the graftable monomer, may simply undergo a thermal loss of a chlorine atom in order to give another unstable structure (see Figure 5).

Allylic chloride (labile structure)
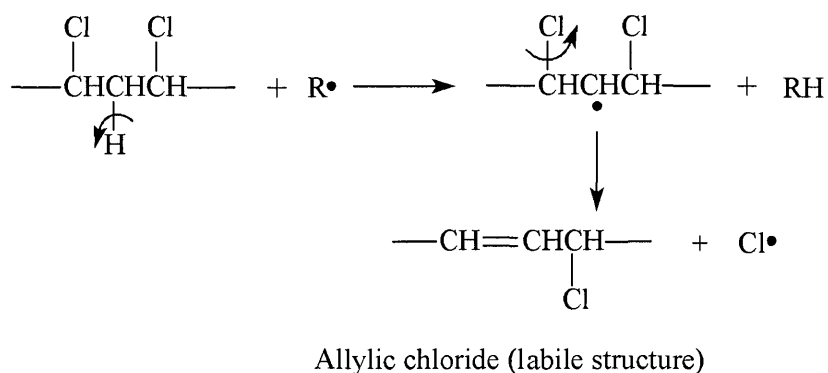
Figure 5. Formation of allylic labile structure

In short, the free-radical grafting on PVC will introduce structural defects that will decrease the thermal stability if they are not removed completely.

Recently, reinitiation from the structural defects of PVC with metal catalysts has been used for living radical graft copolymerization (Figure 6).[10] Usually, Cu(0)/bpy, CuCl/bpy, CuBr/bpy, Cu_2O/bpy, Cu_2S/bpy, and Cu_2Se/bpy (where bpy = 2,2'-bipyridine) were used as catalysts. The following monomers were investigated in these graft copolymerization experiments: methyl methacrylate, butyl methacrylate, *tert*-butyl methacrylate, butyl acrylate, methacrylonitrile, acrylonitrile, styrene, 4-chlorostyrene, 4-methylstyrene, and isobornyl methacrylate.

The results demonstrated that the graft copolymerization can indeed be initiated directly from the structural defects available in the PVC backbone. Therefore, well-

defined PVC graft copolymers can be designed. However, the copolymers are contaminated by the residual metal, and their compositions depend on the number of reactive structural defects in the starting PVC.

$$—CH=CH\overset{\overset{\displaystyle Cl}{|}}{C}H— \quad \xrightarrow{\text{Cu(I) or Cu(0)}} \quad —CH=CH\overset{\bullet}{C}H— \quad \xrightarrow{\text{Monomer}} \quad \text{Propagation}$$

Allylic labile structure

$$—CH_2\overset{\overset{\displaystyle CH_2—}{|}}{\underset{\underset{\displaystyle Cl}{|}}{C}}CH_2— \quad \xrightarrow{\text{CuX/bpy}} \quad —CH_2\overset{\overset{\displaystyle CH_2—}{|}}{\underset{\bullet}{C}}CH_2— \quad \xrightarrow{\text{Monomer}} \quad \text{Propagation}$$
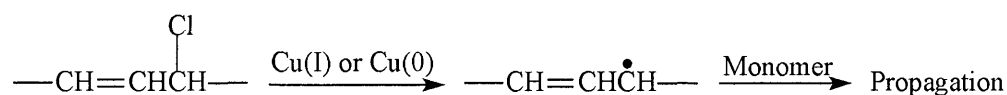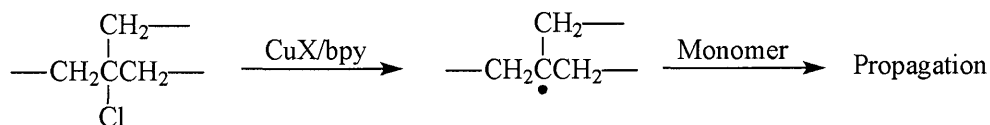
Tertiary chloride structure

Figure 6. Reinitiation from the structural defects of PVC

Thus, three methods[11] for the preparation of graft copolymers are available, but all of these approaches have disadvantages. So it is desirable to find a new approach that does not start from defect sites exclusively and does not produce graft copolymers having low thermal stabilities.

D. New approach to the preparation of graft copolymers from PVC

The current project has provided a new grafting method which involves the relatively unselective homolytic abstraction of chlorine from PVC by metal-centered radical species such as $Bu_3Sn\cdot$. Addition of the resultant C-centered radicals to a graftable

monomer then produces a graft copolymer (Figure 7). However, there is a competition for reaction with monomer between the metal-centered radical and the C-centered radicals from PVC. The main processes are shown in Figure 7,

$$R'_3Me\bullet \xrightarrow[\ k_2\ ]{RX} R'_3MeX + R\bullet \xrightarrow[\ ]{CH_2\!=\!CHY} R(CH_2CH)_nCH_2\overset{\bullet}{C}HY \longrightarrow Copolymer$$

(with Y substituent on the CH group)

$$R'_3Me\bullet \xrightarrow[\ k_1\ ]{CH_2\!=\!CHY} R'_3MeCH_2\overset{\bullet}{C}HY \xrightarrow{CH_2\!=\!CHY} R'_3Me(CH_2CH)_nCH_2\overset{\bullet}{C}HY \longrightarrow Homopolymer$$
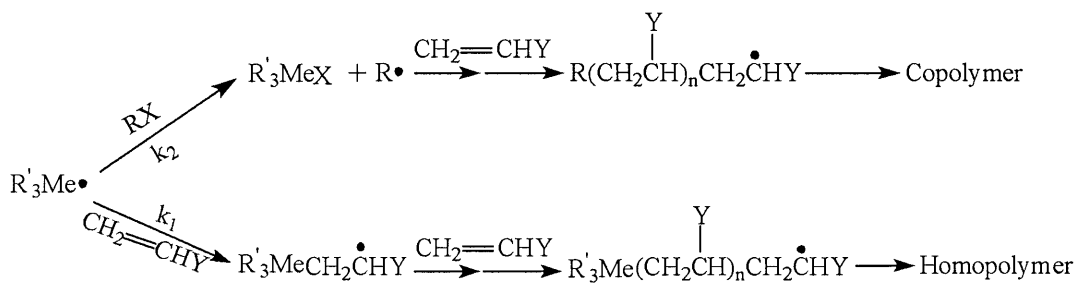
Figure 7. General reaction routes for metal-centered radical

where RX is an aliphatic halide such as PVC; R' is an alkyl group; Me is a metal atom such as tin; the ks are rate constants; and Y represents a variety of groups which will allow the monomers that contain them to polymerize in a radical process.

In order for the grafting reaction to be clean, the initiation of homopolymerization must be unimportant. Two possible ways of overcoming this difficulty are apparent. One is to choose graftable monomers that show relatively low values of k_1. Another is to increase the concentration of PVC relative to that of the monomer.

Successful implementation of the proposed grafting route would be facilitated by the availability of accurate values for the rate constant ratio k_2/k_1. Such information would allow us to select appropriate monomers and PVC:monomer ratios. In order to obtain these important values, a model compound for PVC (a *sec*-alkyl monochloride) and certain monomers would be allowed to react competitively with a large amount of R'_3MeH in the presence of the free-radical initiator azobisisobutyronitrile (AIBN) (see

Figure 8).

From the relative yields of R'_3MeCl and adduct found by GC/MS analysis using an internal standard, it would be possible to obtain the values of k_2/k_1. Graftable monomers with electron-donor groups were more attractive as grafting candidates, owing to their probable lower values of rate constant k_1.

Next, grafting experiments would be carried out with PVC itself. In this case, the metal-centered radical would be produced photolytically from an $R'_3MeMeR'_3$ compound, such as $Bu_3SnSnBu_3$. Any homopolymer formed as a byproduct would be removed from the copolymer by selective solvent extraction.

Finally, the copolymer would be analyzed by gel permeation chromatography (GPC), infrared spectroscopy (IR), and both ^1H and ^{13}C NMR spectroscopy, in order to verify its structure. Then differential scanning calorimetry (DSC) and thermogravimetric analysis (TGA) would be used to study its thermal properties.

RCl: model compound

R'_3MeH: Bu_3SnH
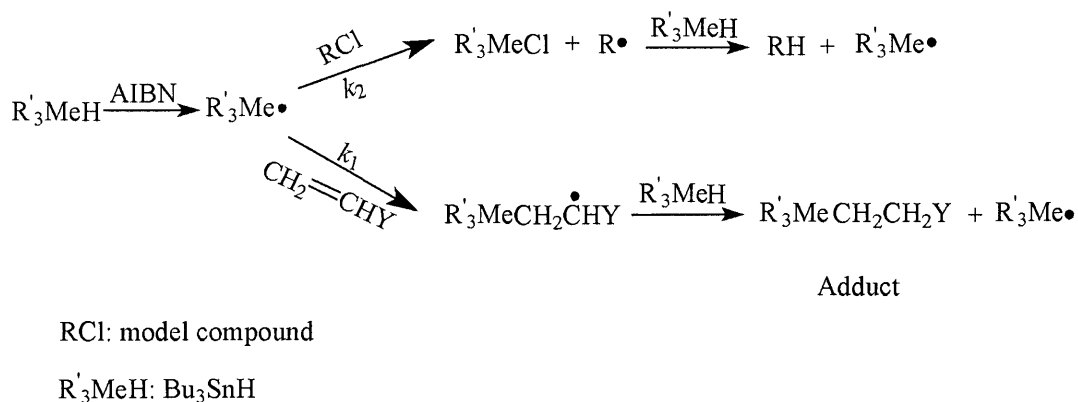
Figure 8. Reaction of the metal-centered radical with

model compound and monomer

II. Experimental

A. Instrumentation

1. Gas chromatography / mass spectroscopy (GC/MS)

A Hewlett-Packard 6890 Series GC instrument equipped with a cross-linked methylsiloxane capillary column (30 m $\times$ 0.25 mm $\times$ 0.25 μm) was used in conjunction with a Hewlett-Packard 5973N Mass Selective Detector. Sample data were analyzed by using Hewlett-Packard 21CFR11 software for the MS ChemStation. The carrier gas was helium.

2. Infrared spectroscopy (IR)

The products were made into films by casting from dilute THF solutions and examined with a Perkin-Elmer 1600 Series FTIR instrument.

3. Melting point determination

Melting points were determined by using a UniMelt (Thomas Hoover) capillary melting point apparatus.

4. Nuclear magnetic resonance (NMR)

The NMR spectra were acquired at ambient temperature with a Varian 400-MHz instrument. Data processing was performed by using Tecmag MacNMR 5.4 software. Chemical shifts are reported in ppm (δ) with TMS (Me$_4$Si) as internal reference

(δ = 0. 00 ppm); chloroform-d and tetrahydrofuran-d_8 were used as solvents.

5. Thermogravimetric analysis (TGA)

All experiments were conducted with a Seiko SSC 5040 Thermal Analysis System. This system included a TG/DTA 200 simultaneous thermogravimetric/differential thermal analyzer with Version 2.0 system software. Sample masses were about 10 mg. The flow rate for nitrogen was 30 mL/min.

6. Differential scanning calorimetry (DSC)

A differential scanning calorimeter consisting of a Perkin-Elmer 7 Series Thermal Analysis System (DSC7) and a TAC7 instrument controller was used to obtain T_g and other characteristics of the polymers.

7. Gel permeation chromatography (GPC)

The data were obtained from the GPC Test 2002 system at the University of Virginia. The system parameters are listed in Table 2-1.

8. Extraction apparatus

A Kontes Soxhlet apparatus equipped with an Allihn condenser and 19 mm $\times$ 90 mm extraction thimbles was used.

9. Solv-Tek Solvent System

Tetrahydrofuran (THF) was purified by passage through the column in a Solv-Tek

Solvent System.

10. UV reactor

The photochemical reactor (Cat. No. RPR-100) was manufactured by the Southern New England Ultraviolet Company. The Rayonet photochemical reactor lamps (Cat. No. RPR-2537A) came from the same supplier.

Table 2-1. System parameters of GPC

System Parameters	
Solvent:	THF
A/D device:	Viscotek T60 A 60Hz
Columns:	Plgel 5 um Mixed
RI name:	Viscotek Model LR40
UV name:	HP VW Detector
Viscometer:	Viscotek Model T60A
Light scattering:	Viscotek Model T60A

B. Materials

2,2'- Azobisisobutyronitrile (AIBN, Fisher, 97%)

Tributyltin chloride (Bu_3SnCl, Aldrich, 96%)

Tributyltin hydride (Bu_3SnH, Aldrich, 97%)

2-Chlorobutane ($CH_3CH(Cl)CH_2CH_3$, Aldrich, 99%)

Vinyl acetate (CH_2=CHOC(O)CH_3, Aldrich, 99%)

Tetrabutyltin (Bu_4Sn, Aldrich, 93%)

Hexa-*n*-butylditin ($Bu_3SnSnBu_3$, Aldrich, 98%)

Chloroform-*d* ($CDCl_3$, Aldrich, 99.8 atom % D)

Tetrahydrofuran-*d*$_8$ (C_4D_8O, Aldrich, 99.5 atom % D)

n-Tridecane (*n*-$C_{13}H_{28}$, Aldrich, 99%)

Tetrahydrofuran (C_4H_8O, Aldrich, 99.9%)

Poly(vinyl acetate) ([-CH_2CH(OC(O)CH_3)-]$_n$, M_w = 167,000 (from GPC), Tg = 30 °C,

Aldrich)

Methanol (CH_3OH, Aldrich, 99.9%)

Poly(vinyl chloride) (PVC, [-CH_2CH(Cl)-]$_n$, Aldrich, M_w = 38,817, M_n = 19,621, M_w/M_n

= 1.98)

n-Pentane ($CH_3(CH_2)_3CH_3$, Fisher, 98%)

Polyisobutylene (PIb, M_w = 4,200,000, M_n = 3,100,000, Aldrich)

Isobutylene (CH_2=C(CH_3)$_2$, Aldrich, 99%)

C. Purification of materials

1. Recrystallization of AIBN

Ten grams of AIBN was dissolved with stirring in 120 mL of boiling methanol. The hot solution was filtered by gravity though a fluted Whatman #4 filter paper and refrigerated overnight. The resulting crystals were separated by suction filtration, washed on the filter with several fresh portions of cold methanol, and dried under vacuum at room temperature for 24 h to give a product melting at 103-105 °C, which is the melting

point reported for the pure substance by Aldrich. This material was stored in the refrigerator prior to use.

2. Purification of THF

Immediately before its use, the THF was purified by passing it through the column in the Solv-Tek Solvent System.

D. Determination of abstraction/addition rate constant ratio for model compound and vinyl acetate

1. Reaction

The reaction was carried out in an airtight system. To a 50-mL one-neck round-bottom flask containing a magnetic stirring bar were added 0.020 g (0.12 mmol) of AIBN, 2.523 g (8.67 mmol) of tributyltin hydride, 1.052 g (12.22 mmol) of vinyl acetate, and 0.581 g (6.28 mmol) of 2-chlorobutane. After three freeze-vacuum-thaw cycles using liquid nitrogen, the flask was heated with stirring for 3 h in a silicone oil bath at 50 ± 3 °C and then cooled to room temperature. Tetrahydrofuran (16.5 mL) and 0.123 g of an internal standard, n-tridecane, were added, and after an additional 20 min of stirring at ice-water temperature, the mixture was analyzed by GC/MS.

The experiment was repeated several times with different Bu_3SnH:vinyl acetate:2-chlorobutane ratios.

2. NMR analysis

Prior to THF addition, product mixtures were analyzed by ^1H and proton-

decoupled ^{13}C NMR spectroscopy in chloroform-d solutions.

3. GC/MS analysis

The GC parameters are shown in Table 2-2.

Table 2-2. GC parameters

GC Parameters
Injector temp.:   160 °C
Detector temp.:   200 °C
Initial temp.:   50 °C
Rate 1:   20 °C /min   From 50 °C to 180 °C
Rate 2:   10 °C /min   From 180 °C to 210 °C
Rate 3:   20 °C /min   From 210 °C to 240 °C
Final temp.:   240 °C
Solvent delay: 5 min

E. Preparation of PVC-g-PVAc

To a quartz flask containing a magnetic stirring bar were added 2.01 g (32.2 mmol monomer units) of PVC, 10.00 g (116.2 mmol) of vinyl acetate, 0.40 g (0.69 mmol) of hexa-n-butylditin, and 105 mL of THF. The flask was stoppered, and the contents were stirred until the PVC dissolved completely. Then the flask was cooled in Dry Ice and the solution was degassed for 25 min with flowing argon, allowed to warm to room

temperature, and irradiated in the UV reactor for 24 h. Following the addition of 50 mL of fresh THF and filtering through paper to remove degraded polymer, the solution was poured into a large excess of methanol, with stirring, and the polymeric product was isolated by suction filtration. It was then redissolved in THF, precipitated again into methanol, recovered by suction filtration, subjected to Soxhlet extraction with methanol for 36 h, and dried under vacuum at 50 °C. The yield was 1.80 g.

F. Characterization of PVC-*g*-PVAc

1. NMR analysis

The copolymer (0.06 g) was dissolved in tetrahydrofuran-d_8 (0.54 g) containing TMS (Me_4Si) as an internal reference. Spectra were recorded at room temperature using 16 scans for the ^1H spectrum and 20,000 scans for the ^{13}C spectrum. For the ^{13}C spectrum, the pulse interval was 3 s, and the pulse angle was 45°.

2. GPC analysis

The operating parameters for the GPC analysis are shown in Table 2-3. The RI traces were obtained from THF solutions on an LR40 laser refractometer. Polymer Labs 5-mm mixed-C columns along with Hewlett-Packard instrumentation (Series 1100 HPLC) and Viscotek software (TriSEC GPC Version 3.0, Viscotek Corp.) were used.

3. FTIR analysis

The samples were made into film by casting from dilute THF solutions. In a typical preparation, 2 mL of THF and 80 mg of graft copolymer or PVC were converted

into a solution by hand swirling, and the solution was allowed to evaporate at room temperature. The resulting film was dried under vacuum at 25 °C and examined at 2 cm^{-1} resolution, using 128 scans.

Table 2-3. Operating parameters for GPC

Operating Parameters

Injection volume (mL): 0.1	Wavelength: 0
Flow rate (mL/min): 1	LS instrument const.: 0
Delay time (min): 0	Incident intensity: 0
Stop time (min): 26	Scattering angle: 0
Inlet pressure (KPa): 44.71	Flory const.: 0
2nd virial coeff.: 0	Refractive index: 0
	Polymer dn/dc: 0

G. Thermal properties of PVC-*g*-PVAc

1. DSC analysis

The following procedure was followed in order to conduct a DSC run. First, the four-component system of the instrument was allowed to warm up while the sample pans were prepared. Sample masses were usually less than 10 mg. When the instrument was ready, values of the operating parameters were entered into the computer. The temperature of the sample was raised from 20 to 100 °C at the rate of 10.0 °C /min, lowered to 20 °C at 10.0 °C /min, and then raised to 100 °C at 10.0 °C /min under a

nitrogen atmosphere. The graphing mode of the computer allowed the run to be observed while in progress.

2. TGA analysis

Polymer samples were weighed on the balance pan of the instrument, and the weights were entered automatically into the computer. Operating parameters were those shown in Table 2-4.

Table 2-4. TGA parameters

Temp. rate (°C /min)	Hold temp. (°C)	Hold time (min)
20	160	0
10	600	5
−20	25	0

At the end of each run, the raw data were converted into ASC II code and then analyzed by Excel.

H. Preparation of PVC-*g*-PIb

To a quartz flask containing a magnetic stirring bar were added 2.01 g (32.2 mmol monomer units) of PVC, 1.00 g (1.73 mmol) of hexa-*n*-butylditin, and 101 mL of THF. The flask was stoppered, and the contents were stirred until the PVC dissolved completely. Then the flask was cooled in Dry Ice, and the solution was degassed for 25 min with flowing argon. Subsequently, isobutylene (9.47 g, 169 mmol) was introduced at

Dry Ice temperature, and after being allowed to warm to room temperature, the flask was irradiated in the UV reactor for 24 h. Following the addition of 50 mL of fresh THF and filtering through paper to remove degraded polymer, the solution was poured into a large excess of methanol, with stirring, and the polymeric product was isolated by suction filtration. It was then redissolved in a very large amount of THF, precipitated again into methanol, recovered by suction filtration, subjected to Soxhlet extraction with n-pentane for 36 h, and dried under vacuum at 50 °C. The yield was 1.40 g.

This polymer was analyzed by GPC, DSC, and TGA as described in Sections IIF and IIG for PVC-g-PVAc.

III. Results and discussion for PVC-*g*-PVAc

A. Reference compound

1. Adduct from tributyltin hydride and vinyl acetate (Figure 9)

$$Bu_3SnH \xrightarrow{AIBN} Bu_3Sn\bullet$$

$$CH_2=CH-O-\overset{\overset{\displaystyle O}{\|}}{C}-CH_3$$

$$\longrightarrow Bu_3SnCH_2\overset{\overset{\displaystyle O}{\overset{\displaystyle \|}{O\overset{\displaystyle \|}{C}CH_3}}}{\underset{|}{C}H\bullet}$$

$$\Bigg\downarrow Bu_3SnH$$

$$Bu_3Sn\bullet$$

$$+$$

$$Bu_3SnCH_2CH_2O\overset{\overset{\displaystyle O}{\|}}{C}CH_3$$

1
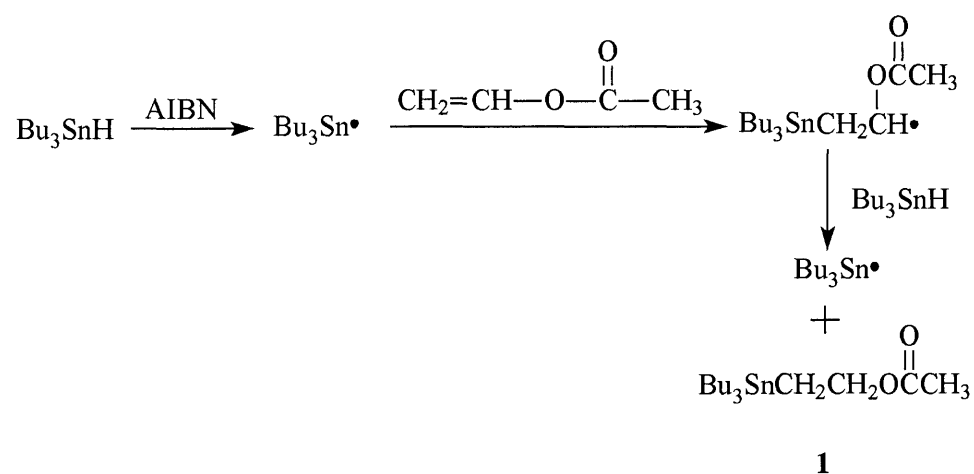
Figure 9. Reaction of tributyltin hydride with vinyl acetate

The GC/MS results for this reaction are shown in Figure 13. In this figure, the peak with a retention time of 6.87 min is tributyltin hydride, because this retention time is the same as that of the pure material in Figure 14. The peak with a retention time of 10.37 min was conclusively identified as adduct 1 with the help of ^{13}C NMR. First we obtained the ^{13}C chemical shift values of *n*-butane from p. 183 of a well-known reference book.[12]

$$CH_3 \text{——} CH_2 \text{——} CH_2 \text{——} CH_3$$

| $\delta =$ | 13.1 | 24.9 | 24.9 | 13.1 | (ppm) |
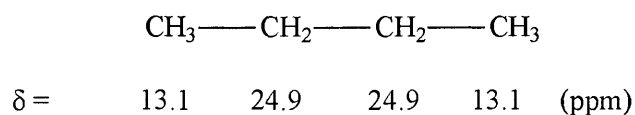
Second, the ^{13}C and ^{1}H NMR spectra of pure tetrabutyltin were recorded as Figures 15

and 16, respectively. With information from p. 298 of reference 12, we could identify the

^{13}C chemical shift values of tetrabutyltin.

$$Bu_3Sn\!\!-\!\!CH_2\!\!-\!\!CH_2\!\!-\!\!CH_2\!\!-\!\!CH_3$$

$$\delta = \qquad 9.04 \quad 29.58 \quad 27.73 \quad 14.06 \quad (ppm)$$
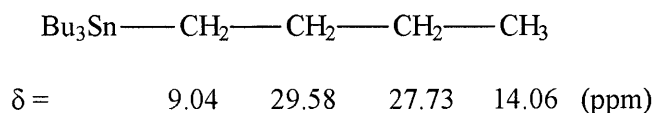
So, the Bu_3Sn- group changed the ^{13}C shifts as follows:

$$\triangle\delta_1 = 9.04 - 13.1 = -4.1 \text{ (ppm)} \qquad \text{(3-1)}$$

$$\triangle\delta_2 = 29.58 - 24.9 = +4.7 \text{ (ppm)} \qquad \text{(3-2)}$$

$$\triangle\delta_3 = 27.73 - 24.9 = +2.8 \text{ (ppm)} \qquad \text{(3-3)}$$

$$\triangle\delta_4 = 14.06 - 13.1 = +1.0 \text{ (ppm)} \qquad \text{(3-4)}$$

Next, the ^{13}C shifts of adduct **1** were predicted from the calculated values. From p. 228 of

reference 12, the ^{13}C shifts of ethyl acetate are:

$$\overset{\displaystyle O}{\underset{\displaystyle }{\overset{\displaystyle \|}{CH_3\!\!-\!\!CH_2\!\!-\!\!O\!\!-\!\!C\!\!-\!\!CH_3}}}$$

$$1 \qquad 2 \qquad\qquad 3 \quad 4$$

$$\delta = \quad 14.2 \quad 60.3 \qquad 170.6 \quad 21.0 \quad (ppm)$$
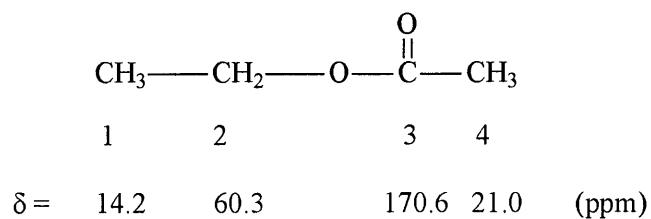
As a result, the δ_1 and δ_2 values for **1** could be calculated:

$$\delta_1 = 14.2 + \triangle\delta_1 = 14.2 + (-4.1) = 10.1 \quad (ppm)$$

$$\delta_2 = 60.3 + \triangle\delta_2 = 60.3 + 4.7 = 65.0 \quad (ppm)$$

So, the chemical shifts of adduct **1** could be predicted as:

$$Bu_3Sn\text{---}CH_2\text{---}CH_2\text{---}O\text{---}\overset{\overset{\displaystyle O}{\|}}{C}\text{---}CH_3$$
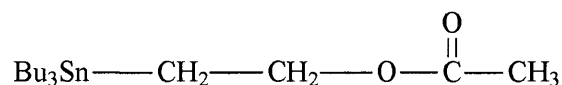
$$\quad\quad\quad\quad 1 \quad\quad 2 \quad\quad\quad 3 \quad 4$$

Predicted values: δ =   10.1   65.0   170.6 21.0 (ppm)

The product of the reaction of tributyltin hydride with vinyl acetate has the ^{13}C NMR spectrum shown in Figure 17. Also, the ^{13}C and ^1H NMR spectra of pure tributyltin hydride are provided in Figures 18 and 19, respectively.

$$Bu_3Sn\text{---}CH_2\text{---}CH_2\text{---}O\text{---}\overset{\overset{\displaystyle O}{\|}}{C}\text{---}CH_3$$
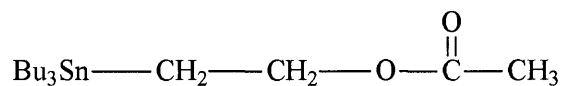
$$\quad\quad\quad\quad 1 \quad\quad 2 \quad\quad\quad 3 \quad 4$$

Actual values: δ =   9.6   65.1   171.3 21.6 (ppm)

Because the predicted and actual ^{13}C shift values are in close agreement, we can draw the firm conclusion that the adduct **1** was indeed formed and that it has a retention time of 10.37 min.

2. Determination of ratio k_2/k_1 in Figure 10

$$\text{Bu}_3\text{SnCl} + \text{H}_3\text{C}\overset{|}{\underset{\text{CH}_2\text{CH}_3}{\text{CH}\bullet}} \xrightarrow{\text{Bu}_3\text{SnH}} \text{H}_3\text{CCH}_2\text{CH}_2\text{CH}_3\uparrow \ (\text{gas})$$

$$\text{Bu}_3\text{Sn}\bullet \xrightarrow{\text{Bu}_3\text{Sn}\bullet} \text{Bu}_3\text{SnSnBu}_3 \quad \mathbf{3}$$

$$\text{Bu}_3\text{SnCH}_2\overset{|}{\underset{\overset{\text{O—CCH}_3}{\underset{\text{O}}{\|}}}{\text{CH}\bullet}} \xrightarrow{\text{Bu}_3\text{SnH}} \text{Bu}_3\text{SnCH}_2\overset{|}{\underset{\overset{\text{O—CCH}_3}{\underset{\text{O}}{\|}}}{\text{CH}_2}} \quad \mathbf{1}$$
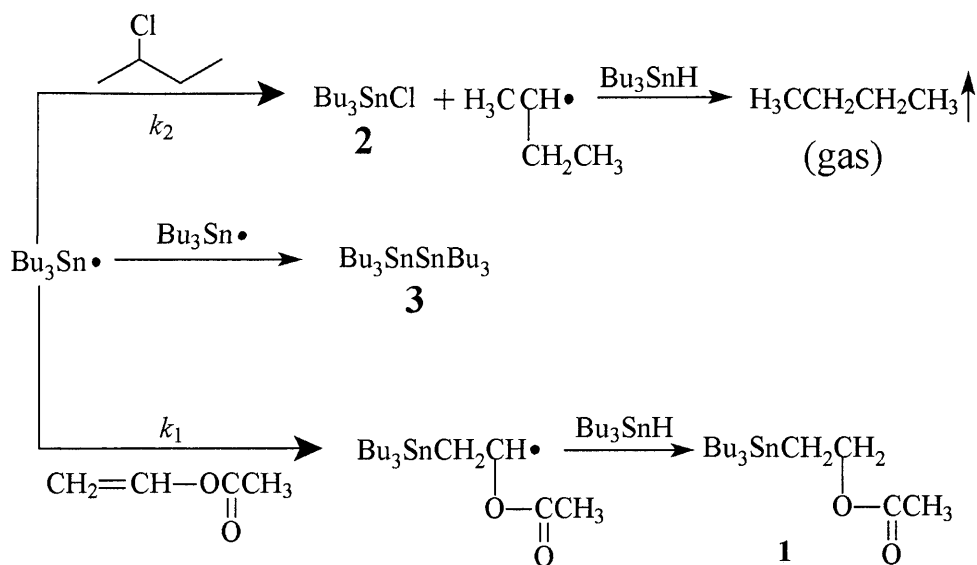
Figure 10. Reaction routes of tributyltin free radical

In this system, the tributyltin free radical will create three products, as shown in Figures 20, 21, and 22. One is adduct **1**, which has the retention time of 10.37 min. The second product is tributyltin chloride, **2**, whose mass spectrum and retention time of 8.67 min are the same as those of pure tributyltin chloride, as depicted in Figure 23. The third product is the dimer **3**, for which the retention time of 11.34 min and the mass spectrum are identical to the results obtained for pure hexa-*n*-butylditin and provided in Figure 24. Because butane is a gas, its yield is difficult to measure accurately. However, tributyltin chloride will remain in the system, and because of the one-to-one stoichiometry, its yield can be used instead for the calculation of k_2/k_1. The equation used to determine this ratio was derived as follows.

Suppose

V = Concentration of vinyl acetate = [vinyl acetate] = [VAc]

R = Concentration of 2-chlorobutane = [2-chlorobutane] = [RCl]

A = Concentration of adduct **1** = [adduct **1**]

B = Concentration of product **2** = [Bu$_3$SnCl]

So,

$$-dV/dt = k_1 V[Bu_3Sn\cdot] \qquad (3\text{-}5)$$

$$-dR/dt = k_2 R[Bu_3Sn\cdot] \qquad (3\text{-}6)$$

Dividing Eq (3-5) by Eq (3-6) and then rearranging gives

$$dV/dR = k_1 V/k_2 R \qquad (3\text{-}7)$$

$$dV/V = (k_1/k_2)\, dR/R \qquad (3\text{-}8)$$

Integrating Eq (3-8) from time = 0 to time t produces

$$\ln(V_t/V_0) = (k_1/k_2)\ln(R_t/R_0) \qquad (3\text{-}9)$$

Figure 10 shows that

$$V_t = V_0 - A \qquad (3\text{-}10)$$

$$R_t = R_0 - B \qquad (3\text{-}11)$$

Owing to the volatility of the small molecules vinyl acetate and 2-chlorobutane, some of these species may be lost after the reaction. Therefore, it is difficult to measure V_t and R_t but easy to determine V_0, R_0, A, and B.

Combination of Eqs (3-9), (3-10), and (3-11) yields

$$k_2/k_1 = \ln(1-B/R_0)/\ln(1-A/V_0) \qquad (3\text{-}12)$$

If the total volume does not change significantly during the reaction, then R_0, B, V_0, and A can be expressed in terms of their weights. The following deductions assume that the total volume remains the same:

If

A_{w0} = Initial weight of vinyl acetate

B_{w0} = Initial weight of 2-chlorobutane

A_w = Weight of adduct **1** after the reaction

B_w = Weight of product **2** after the reaction

$M_{w \text{ (tributyltin chloride)}} = 325.49$ (g/mol)

$M_{w \text{ (2-chlorobutane)}} = 92.57$ (g/mol)

$M_{w \text{ (adduct 1)}} = 377.14$ (g/mol)

$M_{w \text{ (vinyl acetate)}} = 86.09$ (g/mol)

Then

$$B/R_0 = (B_w/M_{w \text{ (tributyltin chloride)}})/(B_{w0}/M_{w \text{ (2-chlorobutane)}})$$

$$= (B_w/B_{w0})(M_{w \text{ (2-chlorobutane)}}/M_{w \text{ (tributyltin chloride)}})$$

$$= 0.2844 \ (B_w/B_{w0}) \tag{3-13}$$

$$A/V_0 = (A_w/M_{w \text{ (adduct 1)}})/(A_{w0}/M_{w \text{ (vinyl acetate)}})$$

$$= (A_w/A_{w0})(M_{w \text{ (vinyl acetate)}}/ M_{w \text{ (adduct 1)}})$$

$$= 0.2283 \ (A_w/A_{w0}) \tag{3-14}$$

If the internal standard *n*-tridecane (GC/MS results shown in Figure 25; the retention time is 6.14 min) or tetrabutyltin (GC/MS results shown in Figure 26; the retention time is 8.74 min) is added into the system after the reaction, then A_w and B_w can

be found from the known weight (W_{IS}) of the internal standard.

For the GC/MS analyses, let us suppose that

P_A = Weight percent of adduct **1**

P_B = Weight percent of tributyltin chloride

P_{IS} = Weight percent of tetrabutyltin or n-tridecane

Then,

$$A_w = (P_A/P_{IS})\, W_{IS} \tag{3-15}$$

$$B_w = (P_B/P_{IS})\, W_{IS} \tag{3-16}$$

Equation (3-12) can now be rewritten as follows:

$$k_2/k_1 = \ln[1 - 0.2844(P_B W_{IS})/(P_{IS} B_{w0})]/\ln[1 - 0.2283(P_A W_{IS})/(P_{IS} A_{w0})] \tag{3-17}$$

The internal standard was tetrabutyltin for the runs in Table 3-1, where

Mole ratio = tributyltin hydride:vinyl acetate:2-chlorobutane.

Table 3-1. Values of k_2/k_1 for different mole ratios of reactants

Mole ratio		A_{w0}	B_{w0}	W_{IS}	P_A (%)	P_B (%)	P_{IS} (%)	k_2/k_1
1:1:1	(Figure 27)	0.51	0.56	0.20	5.40	19.64	47.99	4.19
2:1:1	(Figure 28)	0.62	0.68	0.20	1.58	5.90	13.60	4.31
3:1:1	(Figure 29)	0.52	0.57	0.20	4.74	20.41	16.18	5.17
1.5:1:1	(Figure 30)	0.52	0.57	0.20	3.33	8.94	22.03	3.09

The second set of runs (Table 3-2) used n-tridecane as the internal standard.

Table 3-2. Values of k_2/k_1 for different mole ratios of reactants

Mole ratio		A_{W0}	B_{W0}	W_{IS}	P_A (%)	P_B (%)	P_{IS} (%)	k_2/k_1
3:1:1	(Figure 31)	0.50	0.53	0.113	7.45	18.14	3.51	3.24
3:1.6:1	(Figure 32)	0.81	0.58	0.118	11.28	19.54	3.86	3.39
1.5:1:1	(Figure 33)	0.53	0.57	0.135	6.86	24.70	7.83	4.57
1.5:2:1	(Figure 34)	1.05	0.58	0.123	5.48	8.60	5.67	3.66

As can be seen from the data in the two tables above, the mean value of the rate constant ratio is 3.95 ± 0.61, where the variance is the average deviation. Thus, the conclusion that the tributyltin free radical is more reactive toward the model compound obviously can be reached. As a result, if the amounts of PVC and vinyl acetate are carefully controlled, then the preparation of PVC-*g*-PVAc in similar reactions should be successful.

B. Characterization of PVC-*g*-PVAc

1. ^{13}C and ^{1}H NMR characterization

The ^{1}H and ^{13}C NMR spectra of pure PVC in tetrahydrofuran-d_8 are provided in Figures 35 and 36. In Figure 35, the peaks between 1.9 and 2.5 ppm come from the —CH$_2$—, and the —CH(Cl)— multiplet appears at about 4.2~4.7 ppm. In Figure 36, $\delta_{C1} = 46.2$~47.5 ppm, and $\delta_{C2} = 56.4$~58.5 ppm.

From Figures 37 and 38, the chemical shifts of poly(vinyl acetate) could be obtained and are given in Table 3-3. (The solvent was chloroform-*d*.)

$$-(\!-CH_2\!-\!-\!-CH\!-\!)_n\!-$$
$$\underset{1}{} \quad \underset{2}{}$$
$$\underset{3}{OC(O)}\!-\!\underset{4}{CH_3}$$
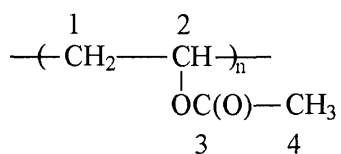
Table 3-3. Chemical shifts of PVAc

	1 (ppm)	2 (ppm)	3 (ppm)	4 (ppm)
^{1}H spectrum	1.5~1.85	4.7~4.9	no H	1.9~2.0
^{13}C spectrum	38.8~40.0	66.1~68.0	170.3	21.1

For the graft copolymer PVC-g-PVAc, obtained as described in Section IIE, the ^{1}H and ^{13}C NMR spectra shown in Figures 39 and 40, respectively, were recorded. The solvent used here was tetrahydrofuran-d_8, and some of the chemical shift data are summarized in Table 3-4.

Table 3-4. Chemical shifts of PVC-g-PVAc

	1 (ppm)	2 (ppm)	3 (ppm)	4 (ppm)
^{1}H spectra	1.5~1.9	4.8~5.2	no H	1.9~2.0
^{13}C spectra	39.5~40.5	66.8~68.6	170.2	20.9

From Tables 3-3 and 3-4, it is apparent that the shifts of the PVAc blocks match well with those of the pure PVAc homopolymer. Hence, the supposed copolymer does indeed contain blocks of PVC and PVAc. Next, calculation of number average molecular weight from the ^{1}H spectrum will be considered, using $M_{w\,pvc}$ as the molecular weight of

the original PVC. In Figure 39, the peaks at $\delta_{pvc} = 4.3 \sim 4.8$ ppm (H) are ascribed to the

—CH(Cl)—, while that at $\delta = 4.8 \sim 5.2$ ppm (also only one H) arises from—CH(O)—.

Therefore, the molecular weight of the PVAc block in the PVC-g-PVAc can be calculated

from Eq (3-18), where I_a and I_b are peak areas,

$$M_{w\,pvac} = (86/62.5)(I_a/I_b)M_{w\,pvc} \qquad (3\text{-}18)$$

and the molecular weight of the PVC-g-PVAc is given by Eq (3-19) .

$$M_{w\,copolymer} = M_{w\,pvc} + M_{w\,pvac} \qquad (3\text{-}19)$$

2. Gel permeation chromatography (GPC) analysis

The PVC-g-PVAc copolymer was analyzed by GPC in THF solution. The GPC

traces showed a monomodal molecular weight distribution and a significant shift of the

peak value toward higher molecular weight. This result strongly suggests that graft

copolymerization occurred without the retention of detectable free PVAc homopolymer

after extraction. Examples of GPC traces are presented in Figure 41. The M_w of PVC is

68,800, and the PVC polydispersity (Pd) is 2.77 according to Figure 41. By using

Eq (3-19) and Figure 39, we obtain a copolymer molecular weight of 115,500. However,

the GPC result is 104,100. The difference between the calculated and GPC results is

probably due, in part, to the nonlinear structure of the graft copolymer.

3. FTIR analysis

Evidence for the PVC-g-PVAc composition also was obtained by FTIR analysis.

The IR spectra of PVC, PVAc, and PVC-g-PVAc are shown in Figures 42, 43, and 44,

respectively. All of these spectra were obtained from solution-cast films. The copolymer

spectrum shows a band at 1747 cm^{-1} that is characteristic for the ester C=O stretch. This result indicates that some of the chloro substituents on the PVC chain were replaced by vinyl acetate groups.

All the results obtained from the NMR, GPC, and FTIR analyses imply that the PVC-*g*-PVAc copolymer was, in fact, prepared by the new method discussed in the Introduction.

C. Thermal properties of PVC-*g*-PVAc

1. Differential scanning calorimetry (DSC) analysis

The differential scanning calorimetry (DSC) analysis of copolymer PVC-*g*-PVAc (in Figure 45) revealed only one glass-transition temperature (T_g) at 46.1 °C, whereas the T_g of the original PVC was 73.3 °C (in Figure 46), and that of PVAc is well-known to be about 30 °C from Aldrich. A single new T_g indicates the absence of PVC and PVAc microphases from the copolymer. This is an expected result, because it is well-documented that PVC is miscible with PVAc.

2. Thermogravimetric analysis (TGA)

The TGA thermograms of PVC, PVC-*g*-PVAc, and PVAc are given in Figure 47.

In the case of PVC, the weight loss starts at 245 °C. Between 245 and 350 °C, a rapid weight loss occurs, and PVC loses 61% of its weight. This loss can be attributed to "zipper" dehydrochlorination. The dehydrochlorination ends at around 420 °C, and the weight loss above that temperature can be attributed to the decomposition of the residual

cross-linked polymer.

In the case of the PVC-*g*-PVAc, the onset of thermal degradation occurs at about 206 °C, owing to the presence of the grafted polymer branch. For the same reason, the weight loss differs from that of the pure PVC between 230 and 320 °C.

In summary, because of the grafted polymer branch, the copolymer became somewhat less stable than the original PVC.

IV. Results and discussion for PVC-*g*-PIb

A. Reference compound

1. Adduct from tributyltin hydride and isobutylene (Figure 11)
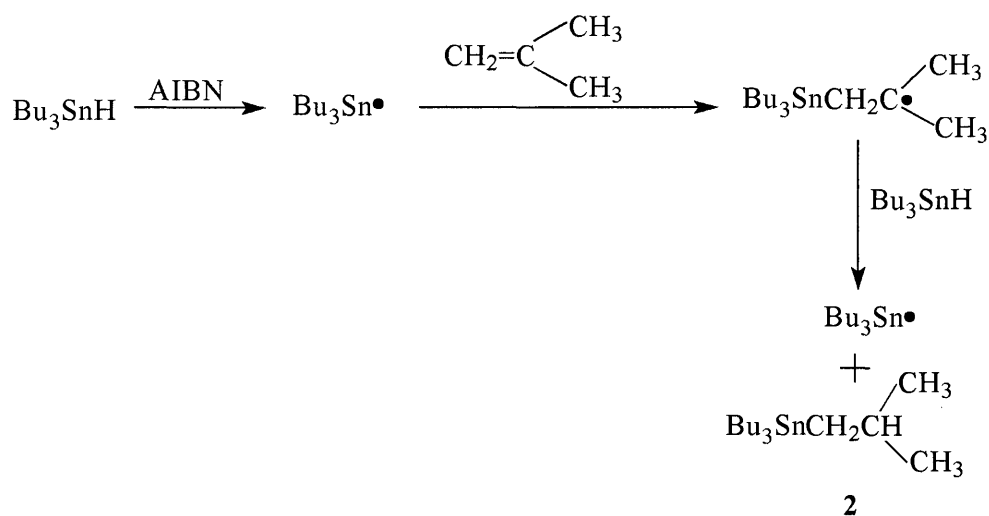
Figure 11. Reaction of tributyltin hydride and isobutylene

As discussed above, the adduct **2** will form in the reaction of tributyltin hydride with isobutylene. The GC/MS results for a product mixture obtained in this way are shown in Figure 48. One of the two peaks is the excess tributyltin hydride (compare Figure 14); the other, with a retention time of 8.48 min, is adduct **2**, as shown by ^{13}C NMR (see Figure 49).

As discussed in Section IIIA, the Bu$_3$Sn- group would change the ^{13}C shifts of an alkyl group as follows:

$$\Delta\delta_1 = 9.04 - 13.1 = -4.1 \text{ (ppm)}$$

$$\Delta\delta_2 = 29.58 - 24.9 = +4.7 \text{ (ppm)}$$

$$\Delta\delta_3 = 27.73 - 24.9 = +2.8 \text{ (ppm)}$$

$$\Delta\delta_4 = 14.06 - 13.1 = +1.0 \text{ (ppm)}$$

The ^{13}C chemical shifts of isobutane, shown below, appear on p. 183 of reference 12.

$$
\begin{array}{c}
\overset{3}{CH_3} \\
| \\
CH_3\text{———}CH\text{———}CH_3
\end{array}
$$

	1	2	3	
$\delta =$	24.6	23.3	24.6	(ppm)
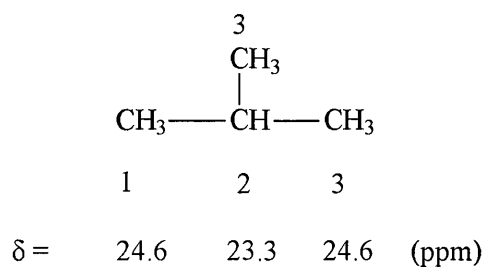
So the predicted and actual ^{13}C chemical shifts of adduct **2** are those listed here:

$$
\begin{array}{c}
\overset{3}{CH_3} \\
| \\
Bu_3SnCH_2\text{———}CH\text{———}CH_3
\end{array}
$$
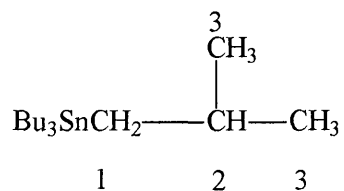
		1	2	3	
Predicted values:	$\delta =$	20.5	28.0	27.4	(ppm)
Actual values:	$\delta =$	21.22	28.18	27.20	(ppm)

(Actual values are from Figure 49.)

The predicted and actual values agree closely enough to justify the conclusion that the product is indeed adduct **2**.

2. Determination of ratio k_2/k_1 in Figure 12

$$\text{Cl} \; (\text{CH}_3)_2\text{CHCH}_2) \xrightarrow{k_2} \text{Bu}_3\text{SnCl} + \text{H}_3\text{C}\overset{\cdot}{\text{C}}\text{H} \xrightarrow{\text{Bu}_3\text{SnH}} \text{H}_3\text{CCH}_2\text{CH}_2\text{CH}_3 \uparrow$$

with CH_2CH_3 branch, (gas)

$$\text{Bu}_3\text{Sn}\cdot \xrightarrow{\text{Bu}_3\text{Sn}\cdot} \text{Bu}_3\text{SnSnBu}_3$$

$$\text{CH}_2\!\!=\!\!\text{C(CH}_3)_2 \xrightarrow{k_1} \text{Bu}_3\text{SnCH}_2\overset{\text{CH}_3}{\underset{\text{CH}_3}{\text{C}}}\cdot \xrightarrow{\text{Bu}_3\text{SnH}} \text{Bu}_3\text{SnCH}_2\text{CH(CH}_3)_2$$
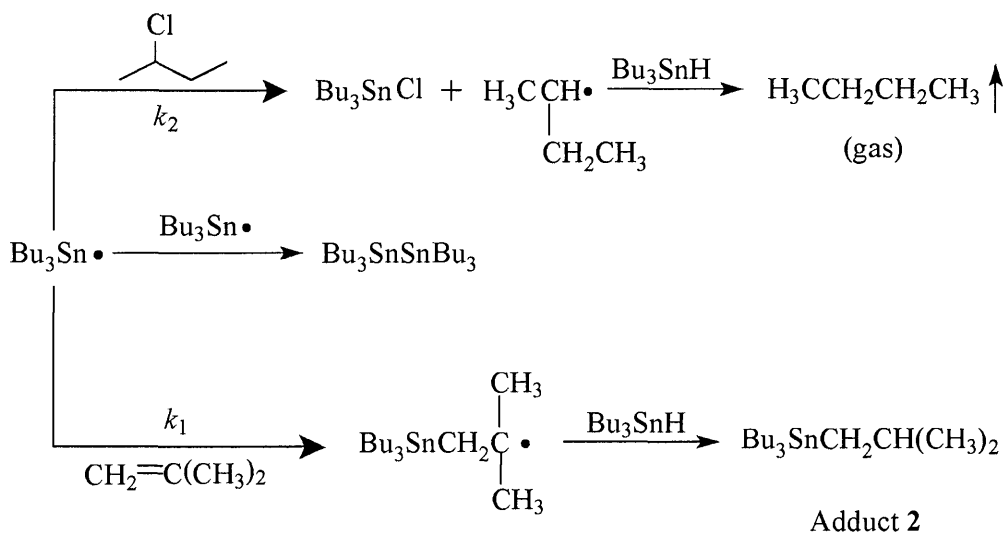
Adduct 2

Figure 12. Reaction routes of tributyltin free radical

In order to be used for the calculation of the ratio k_2/k_1, Eq (3-14) needs minor revision, because the molecular weight $M_{w \text{ (isobutylene)}} = 56$. Thus,

$$A/V_0 = (A_w/M_{w \text{ (adduct 2)}})/(A_{w0}/M_{w \text{ (isobutylene)}})$$

$$= (A_w/A_{w0})(M_{w \text{ (isobutylene)}}/M_{w \text{ (adduct 2)}})$$

$$= 0.1614(A_w/A_{w0}) \tag{4-1}$$

The final equation used to calculate the ratio k_2/k_1 is

$$k_2/k_1 = \ln[1-0.2844(P_BW_{IS})/(P_{IS}B_{w0})]/\ln[1-0.1614(P_AW_{IS})/(P_{IS}A_{w0})] \tag{4-2}$$

Here, all the definitions of parameters are analogous to those in Section III A.

By the use of Eq (4-2), the ratio k_2/k_1 was determined for several sets of reactant mole ratios. The internal standard used was n-tridecane for the runs in Table 4-1, where

Mole ratio = tributyltin hydride:2-chlorobutane:isobutylene.

Table 4-1. Values of k_2/k_1 for different mole ratios of reactants

Mole ratio	A_{W0}	B_{W0}	W_{IS}	P_A (%)	P_B (%)	P_{IS} (%)	k_2/k_1
1:1.6:6.7 (Figure 50)	2.19	0.88	0.119	3.83	46.29	8.53	59.40
1:1.1:8.4 (Figure 51)	2.65	0.58	0.098	0.94	7.60	1.94	71.83
1:1.5:9.1 (Figure 52)	3.01	0.82	0.160	3.85	29.26	12.94	52.39
1:1.4:8.4 (Figure 53)	2.89	0.78	0.093	4.51	44.37	6.28	73.37
1:1.2:8.5 (Figure 54)	2.75	0.62	0.110	4.46	28.67	10.42	54.04
1:1.4:20.2 (Figure 55)	6.56	0.76	0.095	8.50	33.35	6.18	66.19

From the data in the table above, the mean value of the ratio k_2/k_1 for isobutylene is about 62.9 ± 7.6, where the variance is the average deviation. Obviously, the tributyltin free radical, which is well-known to be nucleophilic, reacts much more readily with the model compound than with the isobutylene. Moreover, isobutylene is more reactive than vinyl acetate, because the methyl groups of isobutylene are more strongly electron-donating than the acetoxy group of the vinyl ester. Monomers with electron-donor groups obviously are more attractive as grafting candidates in the process developed here, owing to their relatively slow reaction with the tributyltin free radical.

B. Characterization of PVC-*g*-PIb by GPC

The crude product was a physical mixture of grafted PVC and PIb homopolymer. Isolation of the graft copolymer was achieved by Soxhlet extraction for 36 h with

n-pentane, which removed the homopolymer quantitatively. The PVC-g-PIb copolymer was analyzed by gel permeation chromatography (GPC), using THF as the solvent. The GPC traces (see Figure 56) showed a monomodal molecular weight distribution, which confirmed that the free homopolymer had been removed by extraction with pentane, as well as a lower retention volume compared to that of the original PVC, thereby indicating an increase in the molecular weight. This increase is due to the presence of PIb side chains attached to the parent polymer. The M_w of the original PVC was 68,800, and its polydispersity was 2.77, while the M_w of the copolymer PVC-g-PIb was 95,200, and its polydispersity was 2.28, according to the results in Figure 56.

C. Thermal properties of PVC-*g*-PIb

1. Differential scanning calorimetry (DSC)

In Figure 57, the DSC curve of the PVC-g-PIb does not exhibit a distinct glass-transition temperature (T_g). This result is probably due to the polydispersity of the original PVC and the nonlinear structure of the graft copolymer, which is expected to be an amorphous material containing randomly entangled chains. Also, the curve suggests the presence of a small amount of cross-linking at the higher temperatures and does show an inflection between 25 and 65 °C.

2. Thermogravimetric analysis (TGA)

The TGA thermograms of PVC, PVC-*g*-PIb, and PIb are given in Figure 58.

Above 430 °C, the PIb was decomposed completely. For PVC, the weight loss starts at 230°C . Between 230 and 330 °C, a rapid weight loss occurs, and PVC loses

61% of its weight. This loss can be attributed to dehydrochlorination. In the case of PVC-*g*-PIb, the onset of thermal degradation occurred at about 200 °C, owing to the presence of the grafted polymer branch. The initial weight loss of 58% is lower than that of the pure PVC.

All of these observations suggest that PVC-*g*-PIb was prepared, but in the absence of NMR information, this is not a strong conclusion. Unfortunately, a good NMR solvent for the material could not be identified.
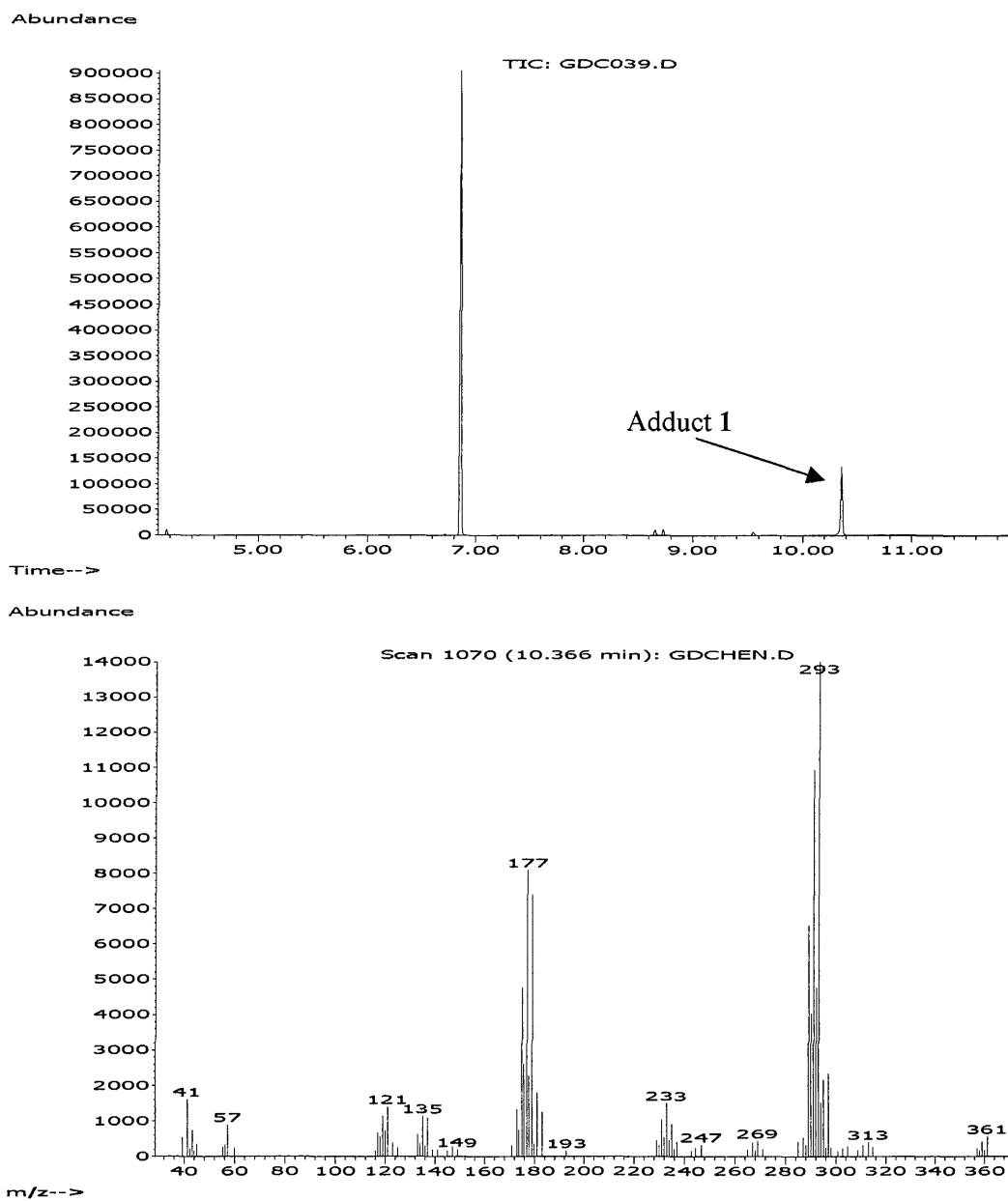
Figure 13. GC/MS results for the reaction products of

tributyltin hydride and vinyl acetate

Abundance

TIC: GDC116.D

3000000

2500000

Bu₃SnH

2000000

1500000

1000000

500000

5.50 6.00 6.50 7.00 7.50 8.00 8.50 9.00 9.50 10.0010.5011.0011.50

Time-->
Abundance

Scan 304 (6.865 min): GDCHEN.D

179

300000
280000
260000
240000
220000
200000
180000
160000
140000   235
120000
100000
80000   121
60000
40000
20000   41
        41   57   135 149   253 269   291
0
   40   60   80   100   120   140   160   180   200   220   240   260   280

m/z-->
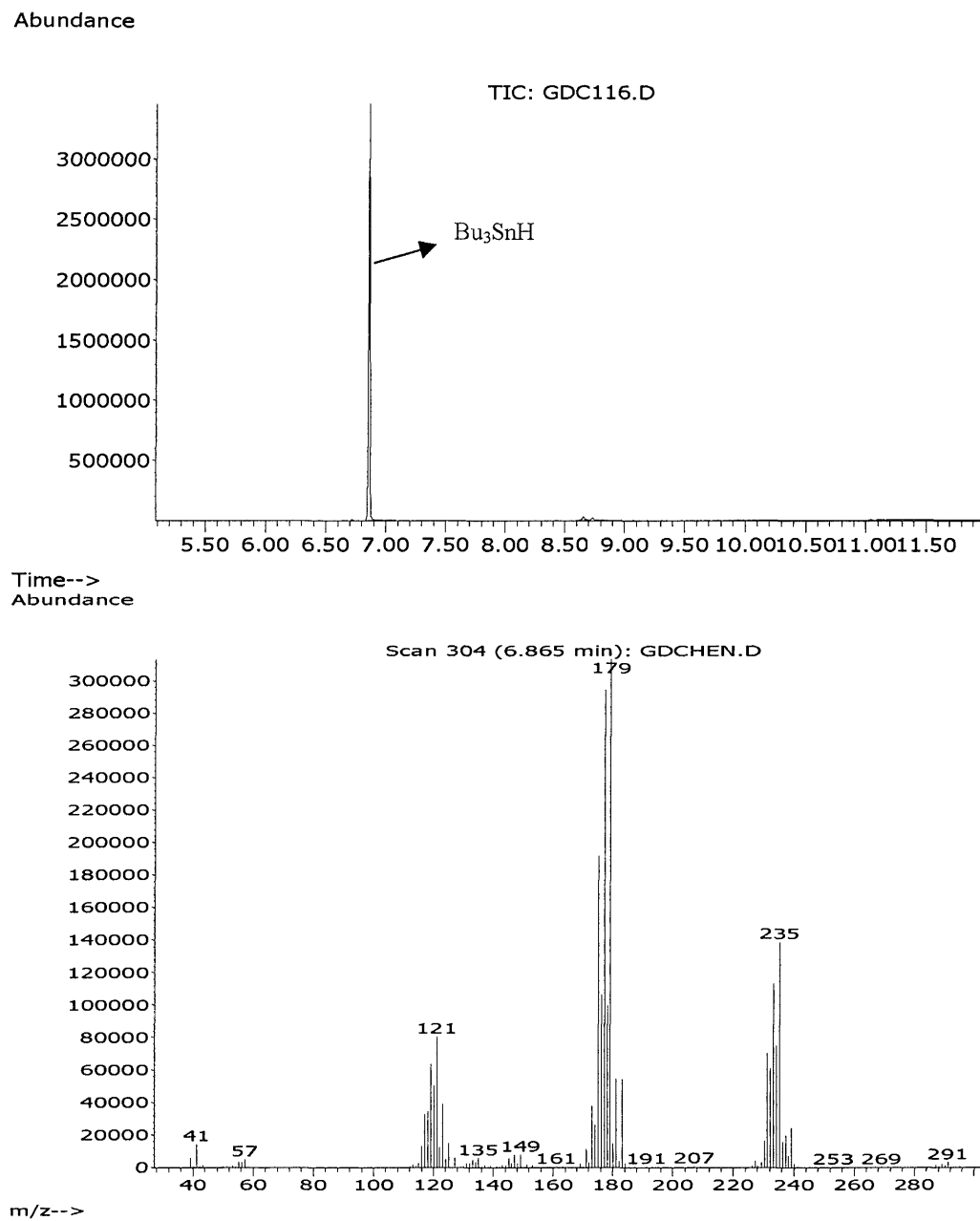
Figure 14. GC/MS results for tributyltin hydride
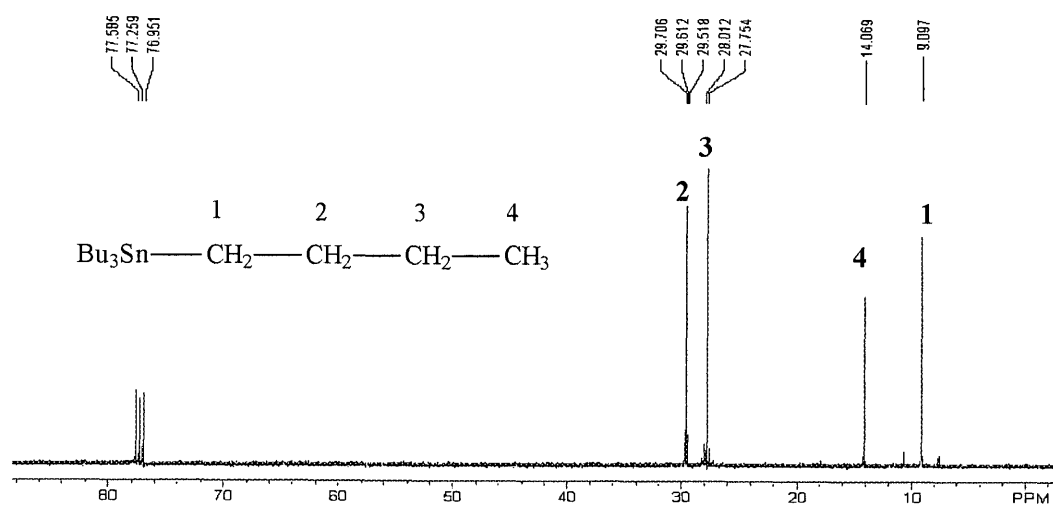
Figure 15. ^{13}C NMR spectrum of tetrabutyltin
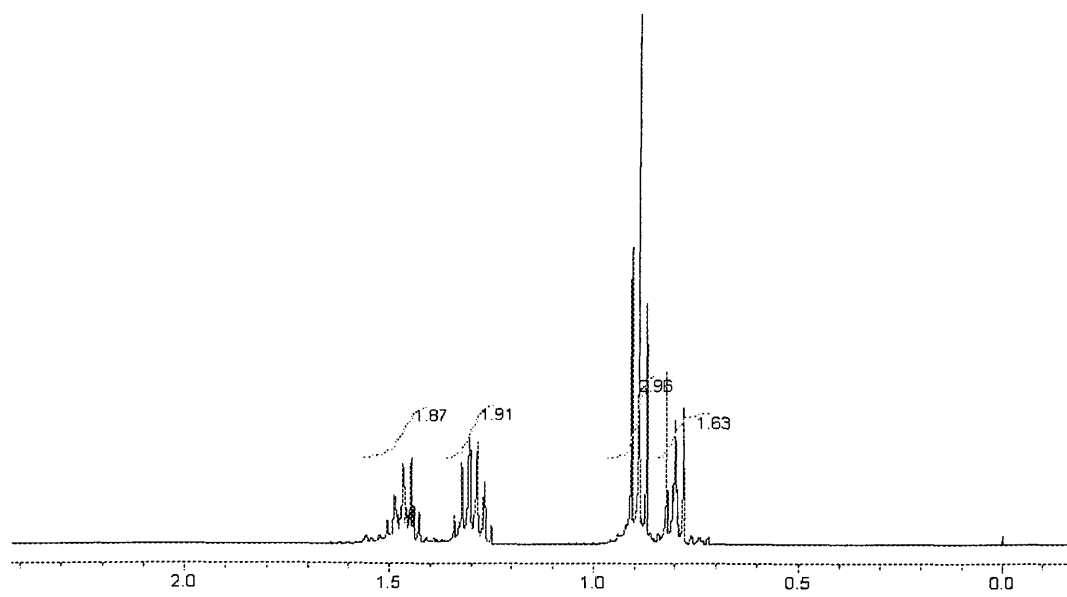
Figure 16. ^{1}H NMR spectrum of tetrabutyltin

171.314

77.609
77.302
76.978
65.093

29.549
29.443
29.341
28.160
27.919
27.647
27.378
21.601
21.585
14.022
9.611
9.593
9.329

O
‖
Bu₃Sn——CH₂——CH₂——O——C——CH₃

1   2   3   4

9.6   65.1   171.3 21.6 (ppm)

200   150   100   50   0 PPM
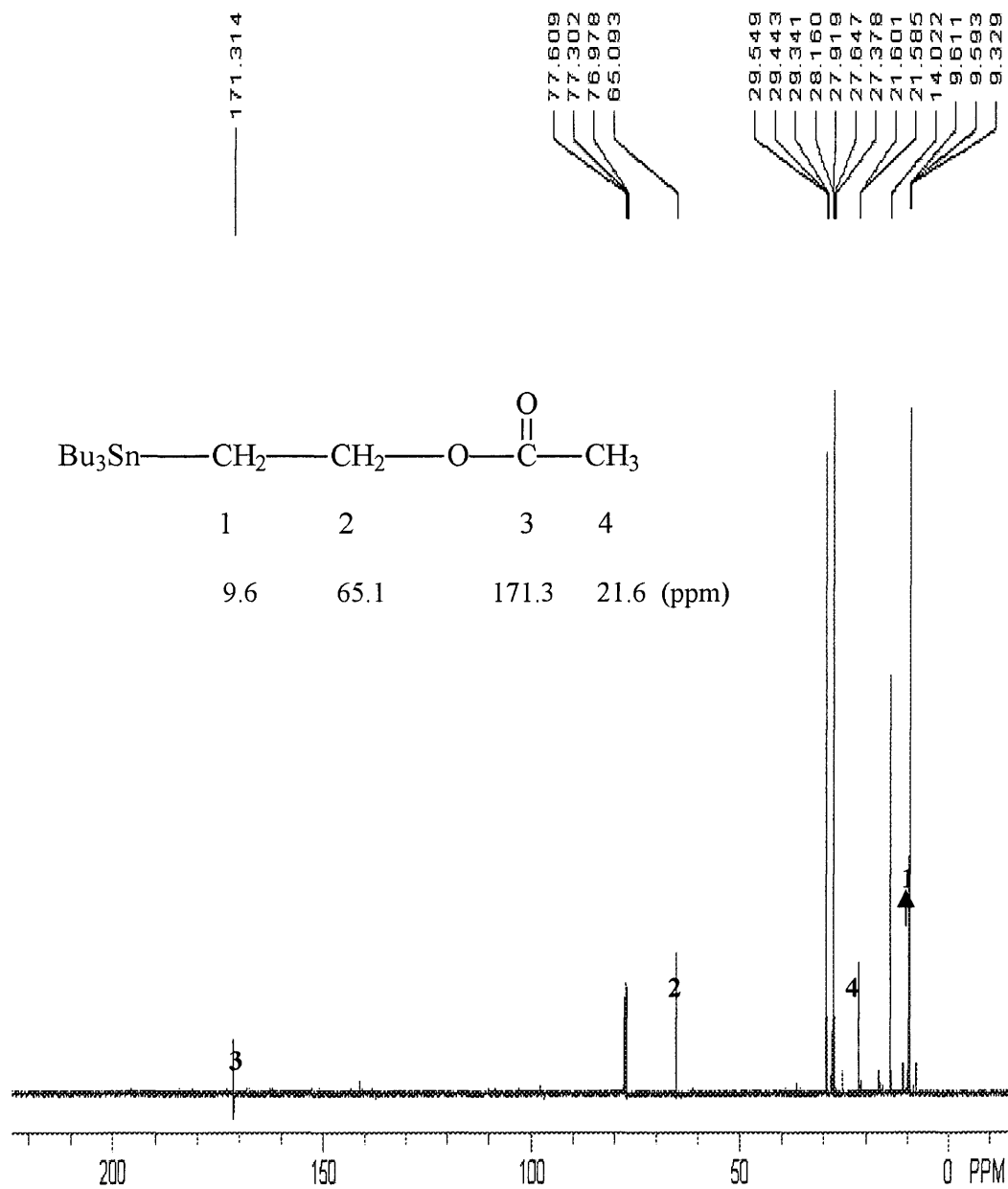
Figure 17. ¹³C NMR spectrum of the reaction product from

tributyltin hydride and vinyl acetate

Bu₃SnH
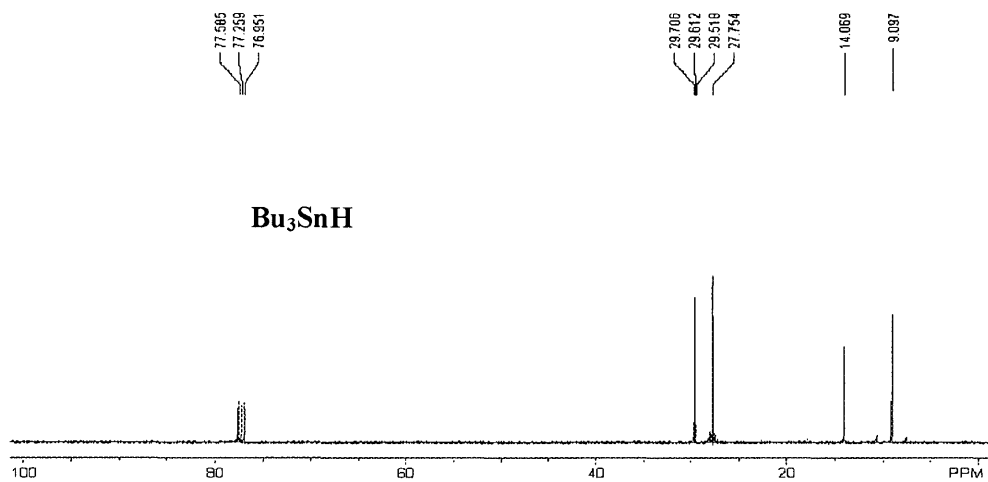
Figure 18. ¹³C NMR spectrum of tributyltin hydride

Bu₃SnH
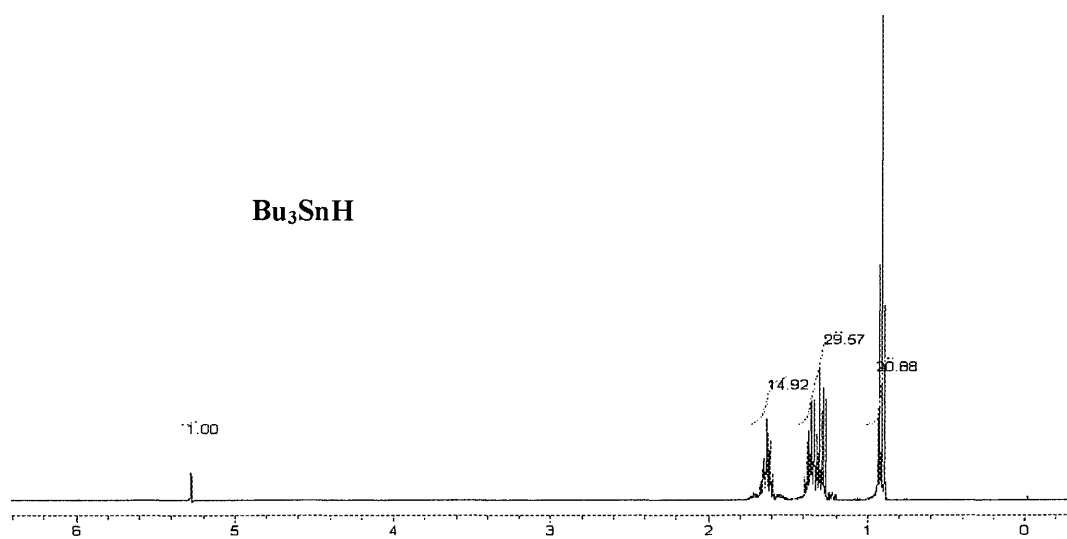
Figure 19. ¹H NMR spectrum of tributyltin hydride

Abundance

TIC: GDC159.D

Time-->

Abundance

Scan 901 (10.373 min): GDCHEN.D

m/z-->
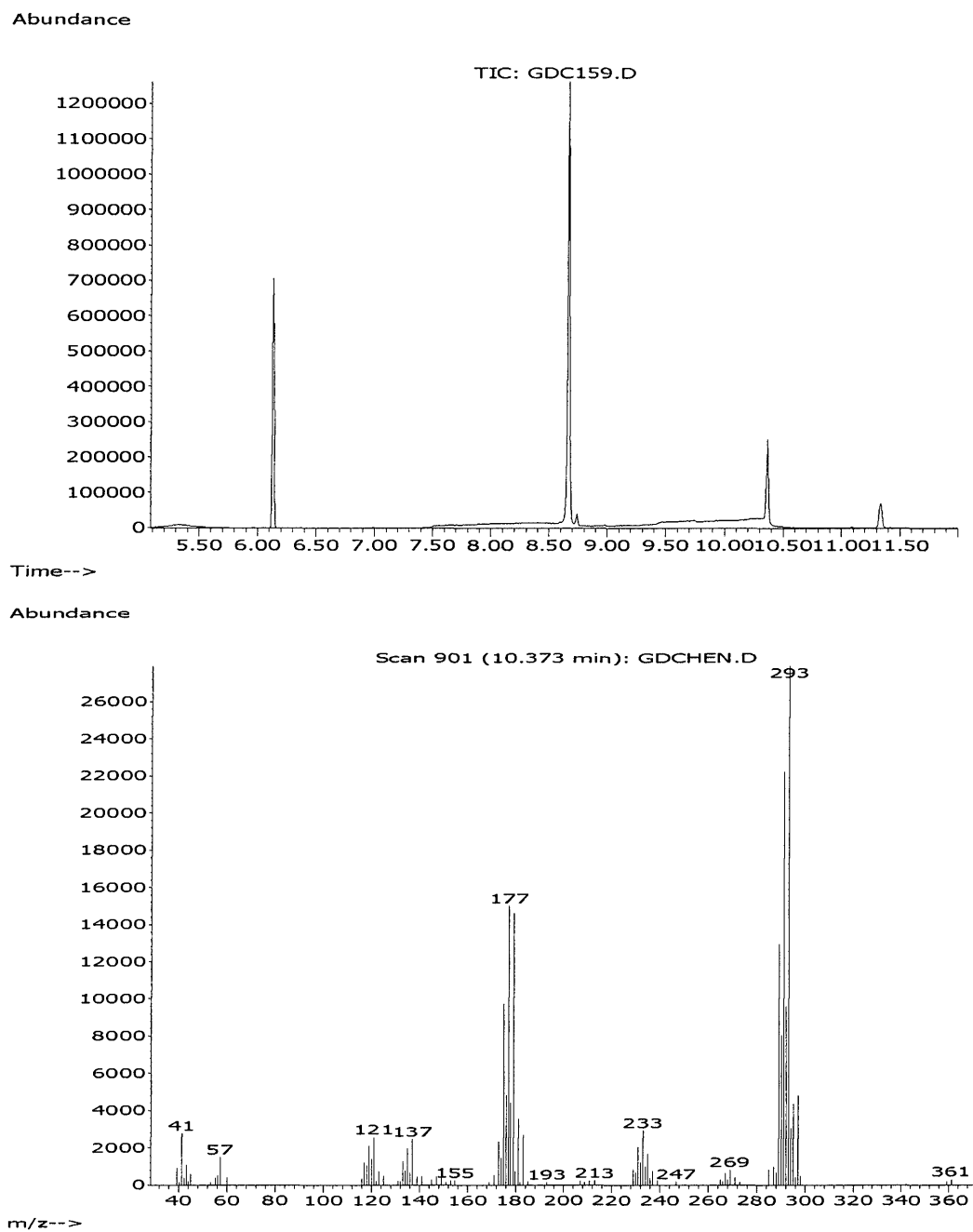
Figure 20. GC/MS identification of adduct **1** from the reaction of

tributyltin hydride and vinyl acetate
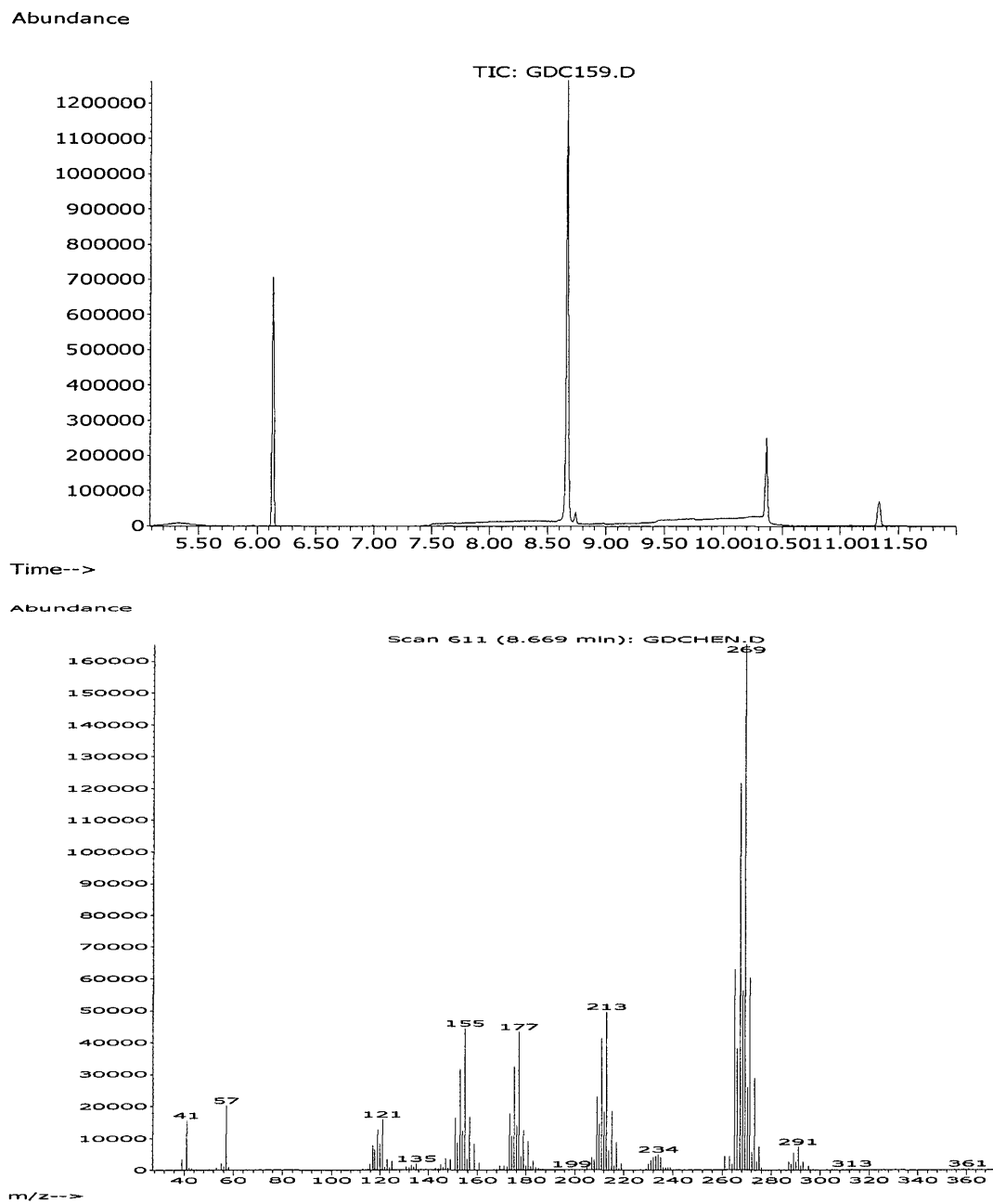
Figure 21. GC/MS results for product **2** from the reaction of

tributyltin hydride and vinyl acetate

Abundance

TIC: GDC159.D

Time-->

Abundance

Scan 1065 (11.337 min): GDCHEN.D

m/z-->
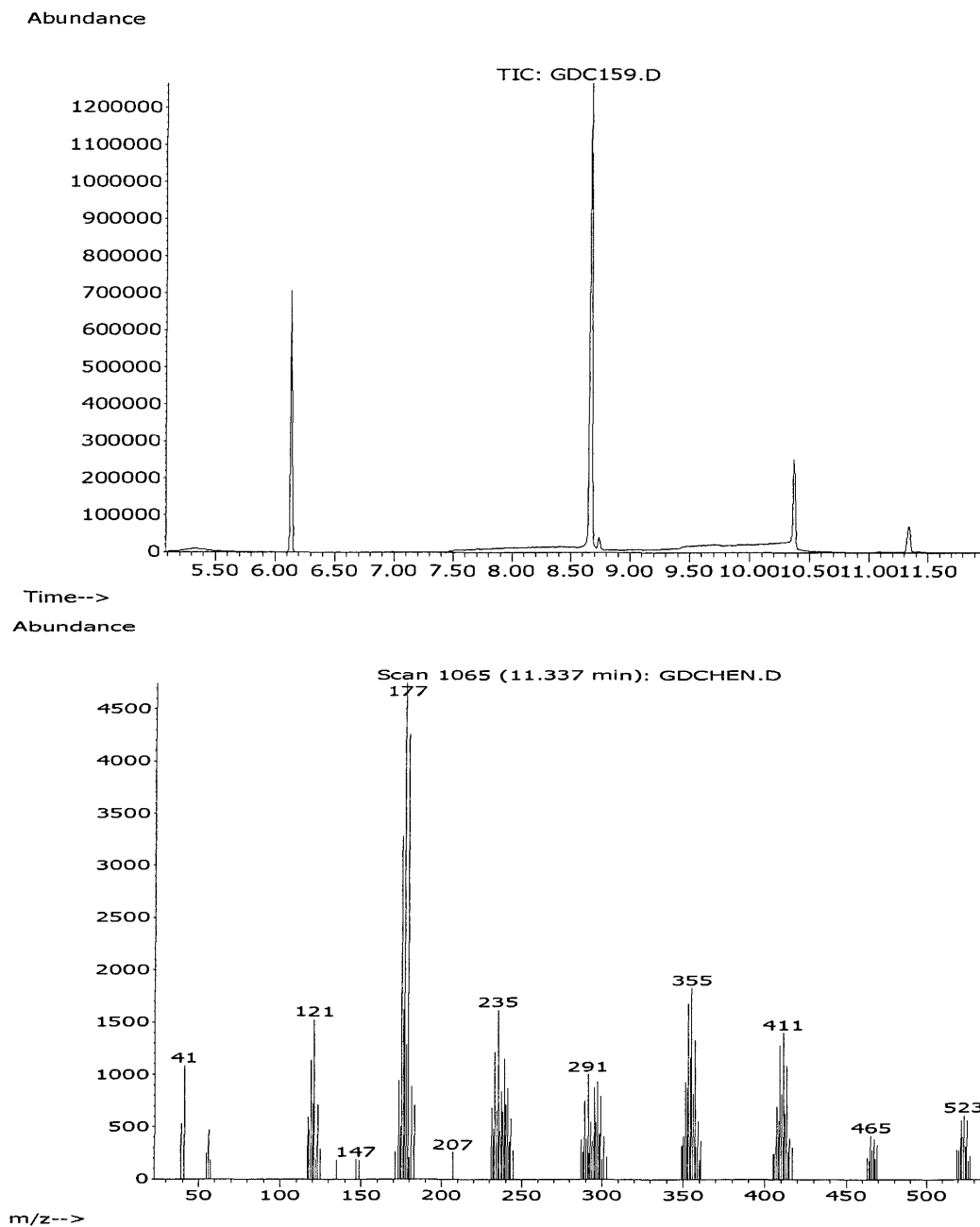
Figure 22. GC/MS results for product **3** from the reaction of

tributyltin hydride and vinyl acetate

Abundance

TIC: GDC031.D

Time-->

Abundance

Scan 100 (8.667 min): GDCHEN.D

m/z-->
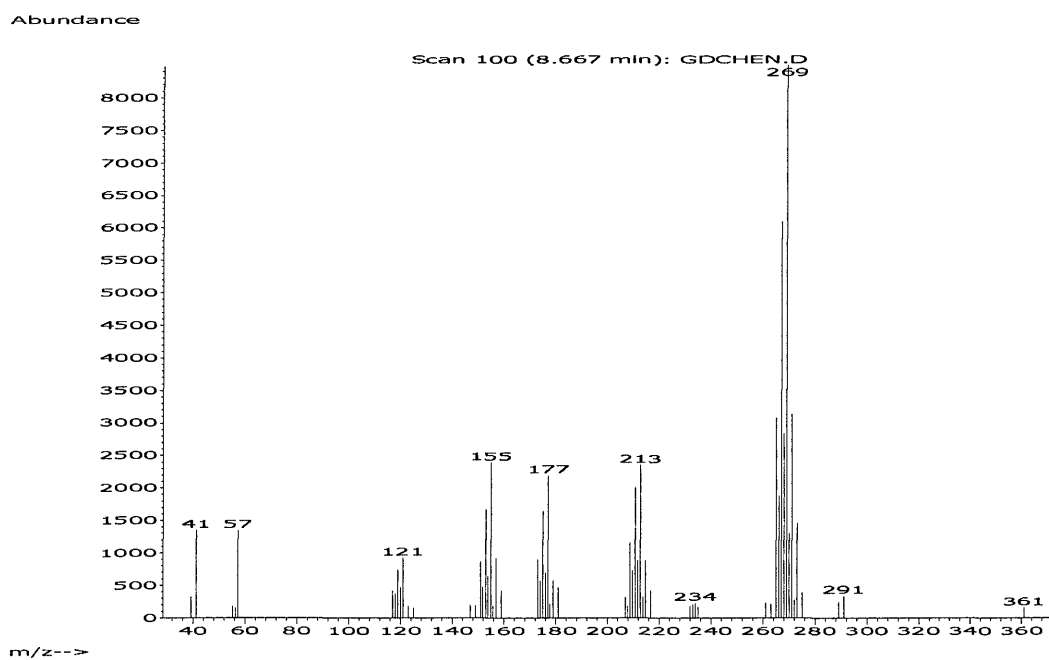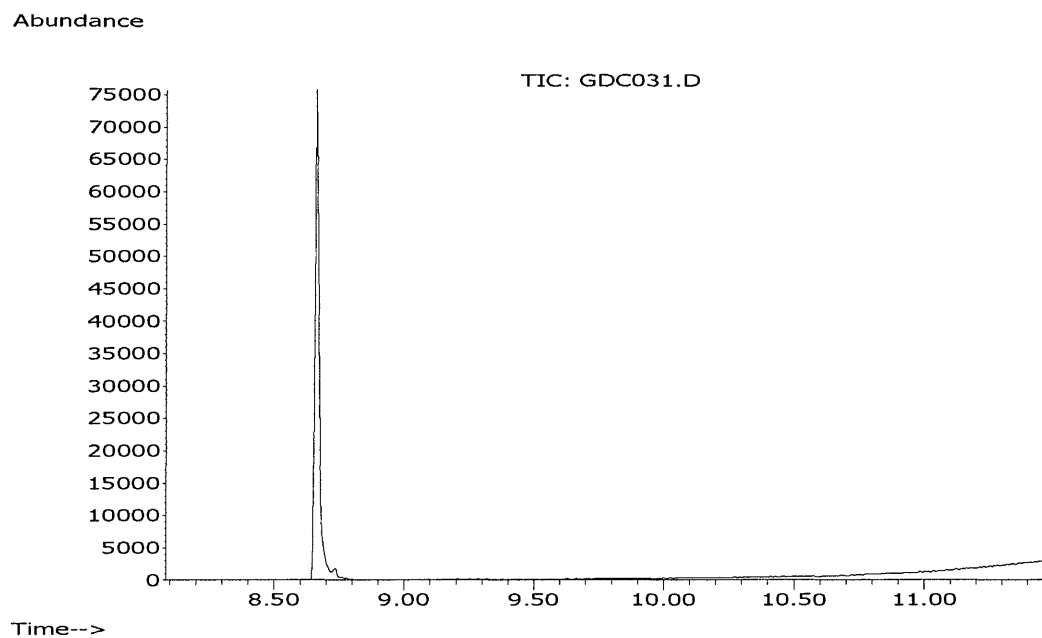
Figure 23. GC/MS results for tributyltin chloride

Abundance

TIC: GDC113.D

1500000
1400000
1300000
1200000
1100000
1000000
900000
800000
700000
600000
500000
400000
300000
200000
100000

5.50 6.00 6.50 7.00 7.50 8.00 8.50 9.00 9.50 10.0010.5011.0011.50

Time-->

Abundance

Scan 1068 (11.354 min): GDCHEN.D
177

75000
70000
65000
60000
55000
50000
45000
40000   355
35000   411
30000   235
25000   121   291
20000   523
15000   467
10000   41
5000   73 96   149   207   257   313
0

50   100   150   200   250   300   350   400   450   500

m/z-->

Figure 24. GC/MS results for hexa-*n*-butylditin

Abundance

TIC: GDCTRIDECANE.D

1e+07

9000000

8000000

7000000

6000000

5000000

4000000

3000000

2000000

1000000

5.50 6.00 6.50 7.00 7.50 8.00 8.50 9.00 9.50 10.0010.5011.0011.50

Time-->

Abundance

Scan 181 (6.143 min): GDCHEN.D

2000000

1900000

1800000

1700000

1600000

1500000

1400000

1300000

1200000

1100000

1000000

900000

800000

700000

600000

500000

400000

300000

200000

100000

0

57

71

43

85

99

112

127

141

155

169

184

207

30 40 50 60 70 80 90 100 110 120 130 140 150 160 170 180 190 200 210

m/z-->

Figure 25. GC/MS results for *n*-tridecane

Abundance

TIC: TBT.D

8000000

7000000

6000000

5000000

4000000

3000000

2000000

1000000

5.50 6.00 6.50 7.00 7.50 8.00 8.50 9.00 9.50 10.0010.5011.0011.50

Time-->

Abundance

Scan 623 (8.739 min): GDCHEN.D

700000   179

650000   235

600000   291

550000

500000

450000

400000

350000

300000

250000   121

200000

150000

100000

50000   41
              57
                   73 91   149   205   261   327 355   405

40 60 80 100 120 140 160 180 200 220 240 260 280 300 320 340 360 380 400

m/z-->

Figure 26. GC/MS results for tetrabutyltin

Abundance

TIC: GDC054.D

Abundance

Scan 1069 (10.360 min): GDCHEN.D

Figure 27. GC/MS results for products from mole ratio = 1:1:1

Abundance

TIC: GDC055.D

1200000
1150000
1100000
1050000
1000000
950000
900000
850000
800000
750000
700000
650000
600000
550000
500000
450000
400000
350000
300000
250000
200000
150000
100000
50000
0

Time-->

5.00   6.00   7.00   8.00   9.00   10.00   11.00

Abundance

Scan 1070 (10.366 min): GDCHEN.D

6000
5500
5000
4500
4000
3500
3000
2500
2000
1500
1000
500
0

293
177
41
57
121
135
233
269

m/z-->

40   60   80   100   120   140   160   180   200   220   240   260   280   300
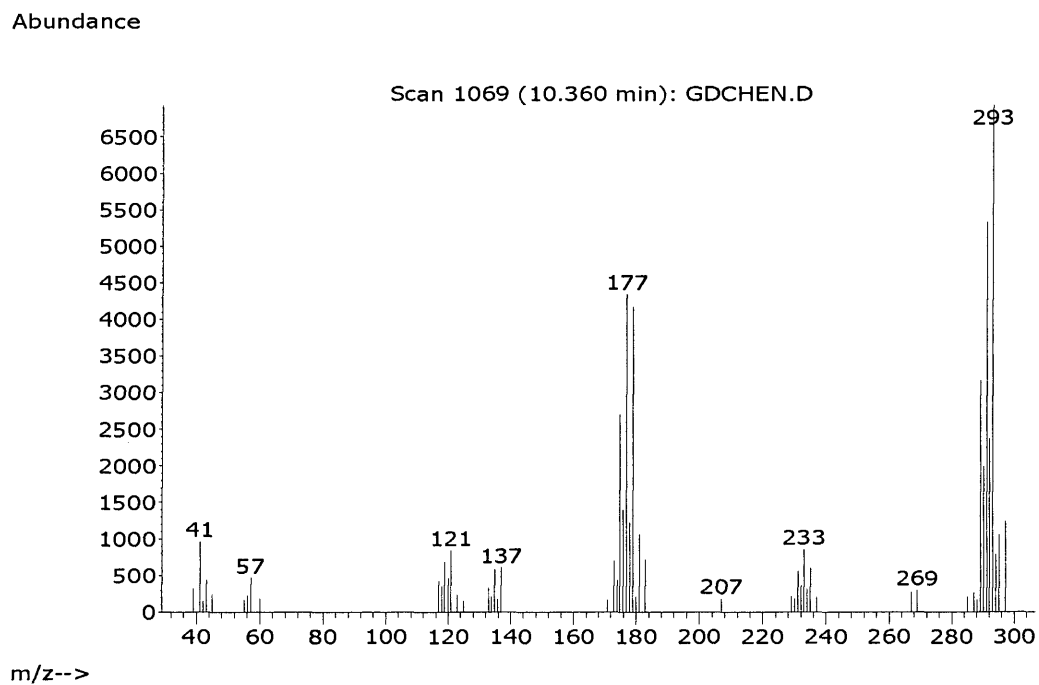
Figure 28. GC/MS results for products from mole ratio = 2:1:1

Abundance

TIC: GDC053.D

```
1200000
1150000
1100000
1050000
1000000
 950000
 900000
 850000
 800000
 750000
 700000
 650000
 600000
 550000
 500000
 450000
 400000
 350000
 300000
 250000
 200000
 150000
 100000
  50000
      0
```

Time-->

          5.00   6.00   7.00   8.00   9.00   10.00   11.00

Abundance

Scan 1069 (10.360 min): GDCHEN.D

```
18000
17000
16000
15000
14000
13000
12000
11000
10000
 9000
 8000
 7000
 6000
 5000
 4000
 3000
 2000
 1000
    0
```

293

177

41   57   121 137   155   193 213   233   247   269   313   361

m/z-->

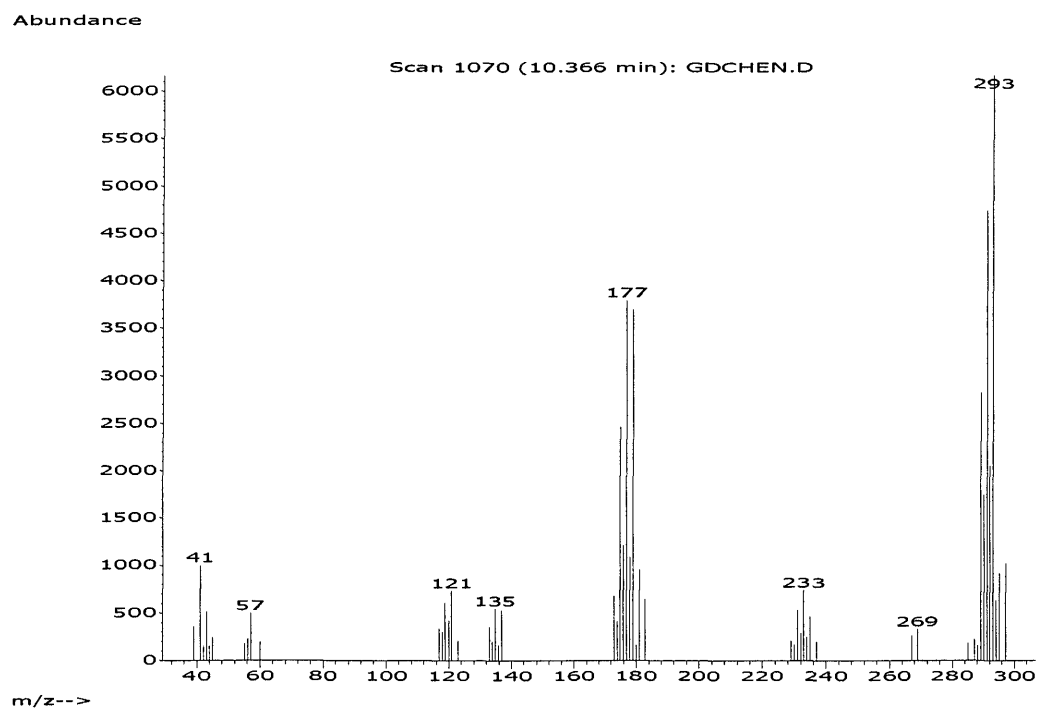   40 60 80 100 120 140 160 180 200 220 240 260 280 300 320 340 360
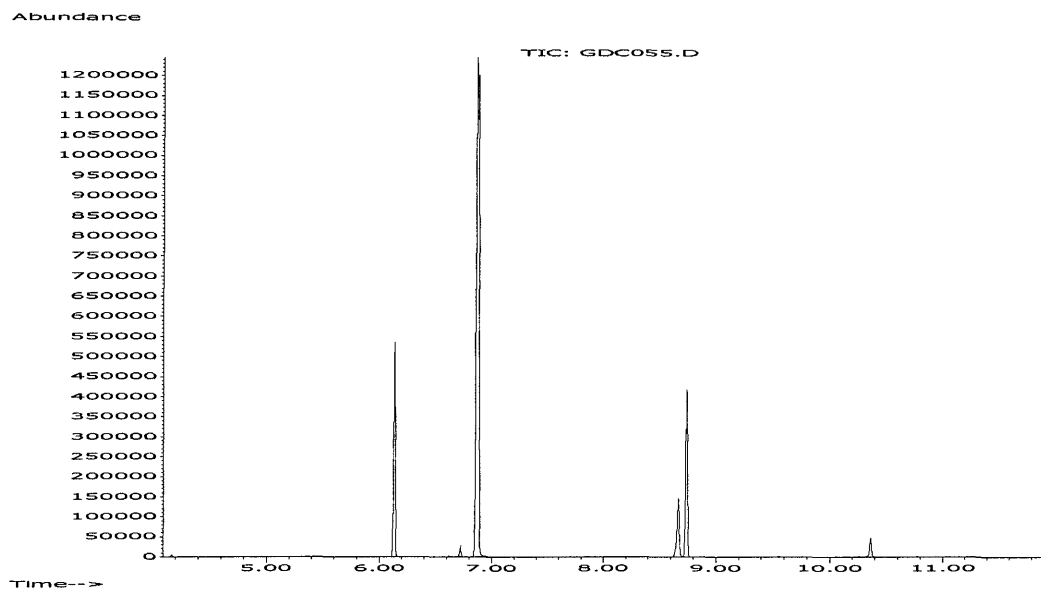
Figure 29. GC/MS results for products from mole ratio = 3:1:1

Abundance

TIC: GDC119.D

5000000
4500000
4000000
3500000
3000000
2500000
2000000
1500000
1000000
500000

5.50 6.00 6.50 7.00 7.50 8.00 8.50 9.00 9.50 10.0010.5011.0011.50

Time-->

Abundance

Scan 901 (10.373 min): GDCHEN.D

293

55000
50000
45000
40000
35000   177
30000
25000
20000
15000
10000   41   121   233   269
5000   57   137   207
         96   155   193   247   313   361
0
40 60 80 100 120 140 160 180 200 220 240 260 280 300 320 340 360

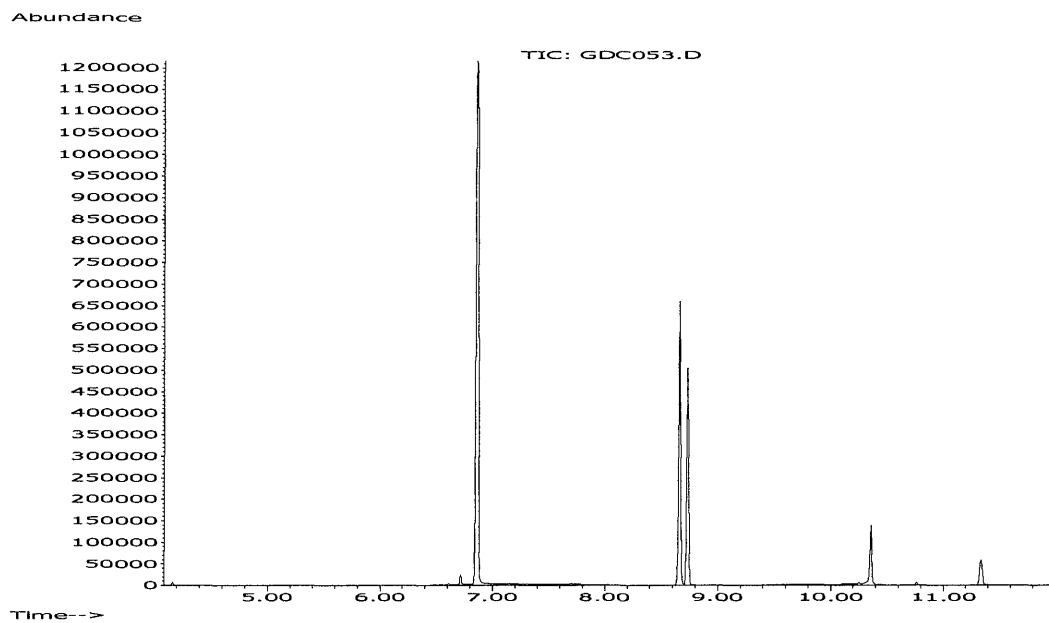m/z-->

Figure 30. GC/MS results for products from mole ratio = 1.5:1:1

Abundance

TIC: GDC183.D

```
2000000
1800000
1600000
1400000
1200000
1000000
 800000
 600000
 400000
 200000
       0
```

Time-->

```
        1.00  2.00  3.00  4.00  5.00  6.00  7.00  8.00  9.00  10.00 11.00
```

Abundance

Scan 1742 (10.374 min): GDCHEN.D

```
85000                                                                293
80000
75000
70000
65000
60000
55000
50000
45000
40000                              177
35000
30000
25000
20000
15000
10000                                       233
 5000   41                   121137                      269
      57                       155   193 213    249              361
     40  60  80  100 120 140 160 180 200 220 240 260 280 300 320 340 360
```

m/z-->

Figure 31. GC/MS results for products from mole ratio = 3:1:1

Abundance

TIC: GDC188.D

2000000
1800000
1600000
1400000
1200000
1000000
800000
600000
400000
200000

5.50 6.00 6.50 7.00 7.50 8.00 8.50 9.00 9.50 10.0010.5011.0011.50

Time-->

Abundance

Scan 900 (10.367 min): GDCHEN.D

120000   293
110000
100000
90000
80000
70000   177
60000
50000
40000
30000
20000   233
10000 41   57   121 137   251 269
    0   149 163   193 207

40   60   80   100 120 140 160 180 200 220 240 260 280 300

m/z-->

Figure 32. GC/MS results for products from mole ratio = 3:1.6:1

Abundance

TIC: GDC172.D

2000000
1800000
1600000
1400000
1200000
1000000
800000
600000
400000
200000

5.50 6.00 6.50 7.00 7.50 8.00 8.50 9.00 9.50 10.0010.5011.0011.50

Time-->

Abundance

Scan 899 (10.361 min): GDCHEN.D

293

60000
55000
50000
45000
40000
35000   177
30000
25000
20000
15000
10000
5000   41   57   121 137   233
0   91   149 163   193 213   251 269

40 60 80 100 120 140 160 180 200 220 240 260 280 300

m/z-->

Figure 33. GC/MS results for products from mole ratio = 1.5:1:1

Abundance

TIC: GDC170.D

2000000
1800000
1600000
1400000
1200000
1000000
800000
600000
400000
200000
0

1.00 2.00 3.00 4.00 5.00 6.00 7.00 8.00 9.00 10.00 11.00

Time-->

Abundance

Scan 1742 (10.371 min): GDCHEN.D

120000
110000
100000
90000
80000
70000
60000
50000
40000
30000
20000
10000
0

293

177

233

41 57   121137   153   193 213   249 269   313   361

40 60 80 100 120 140 160 180 200 220 240 260 280 300 320 340 360

m/z-->

Figure 34. GC/MS results for products from mole ratio = 1.5:2:1

Figure 35. ^{1}H NMR spectrum of original PVC
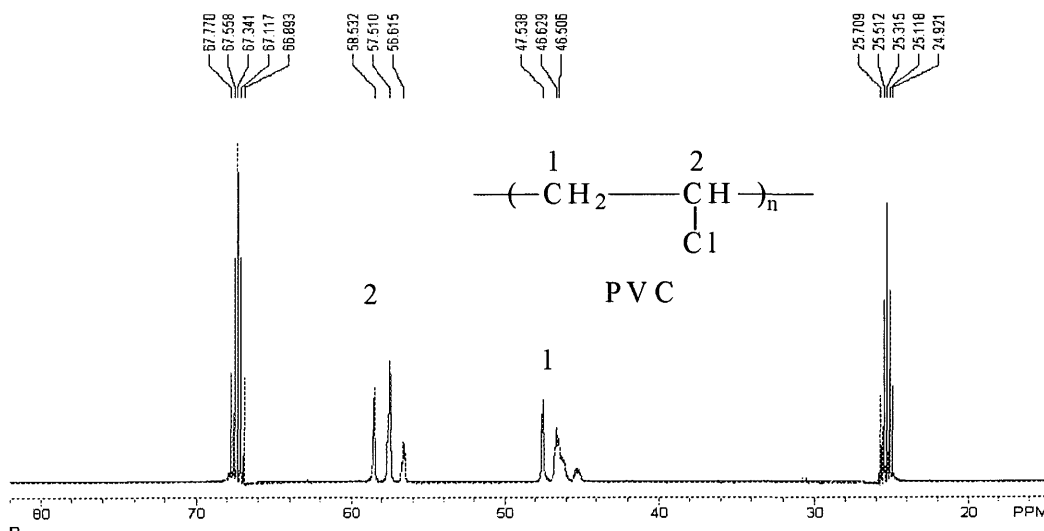
Figure 36. ^{13}C NMR spectrum of original PVC
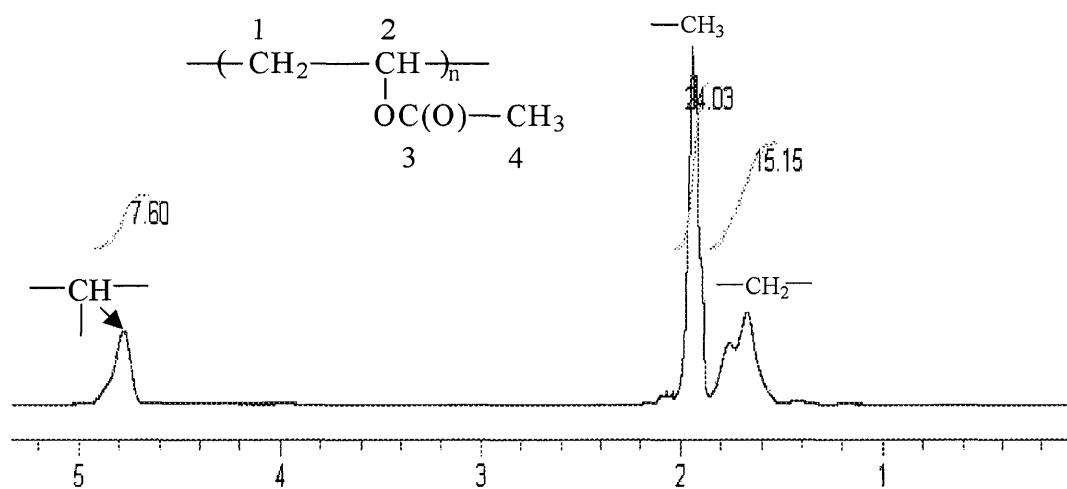
Figure 37. ^1H NMR spectrum of PVAc
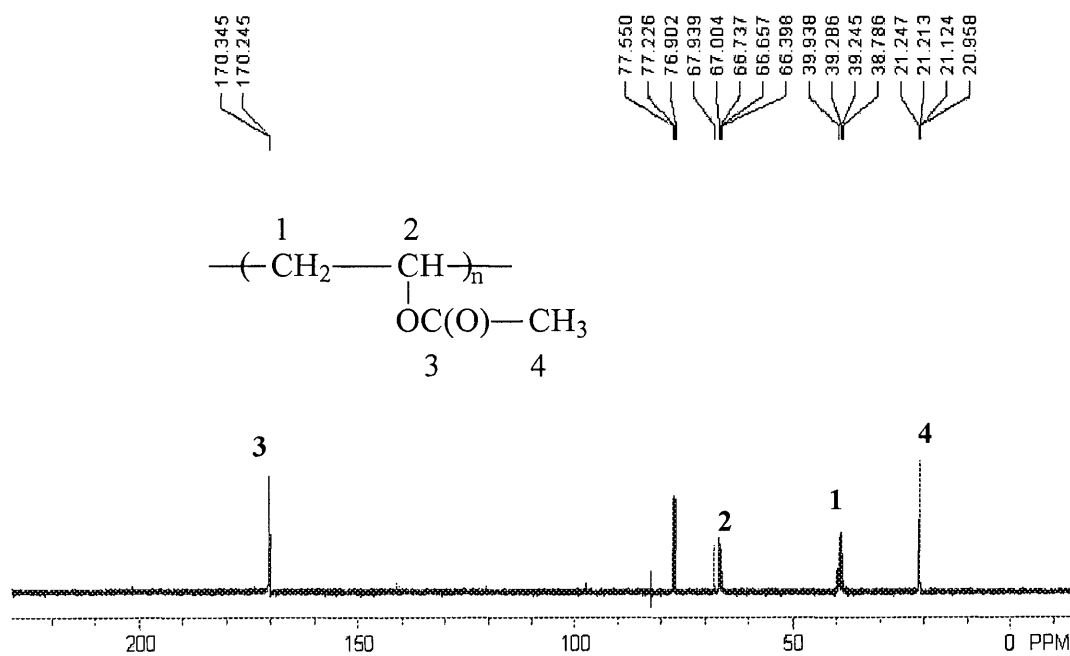
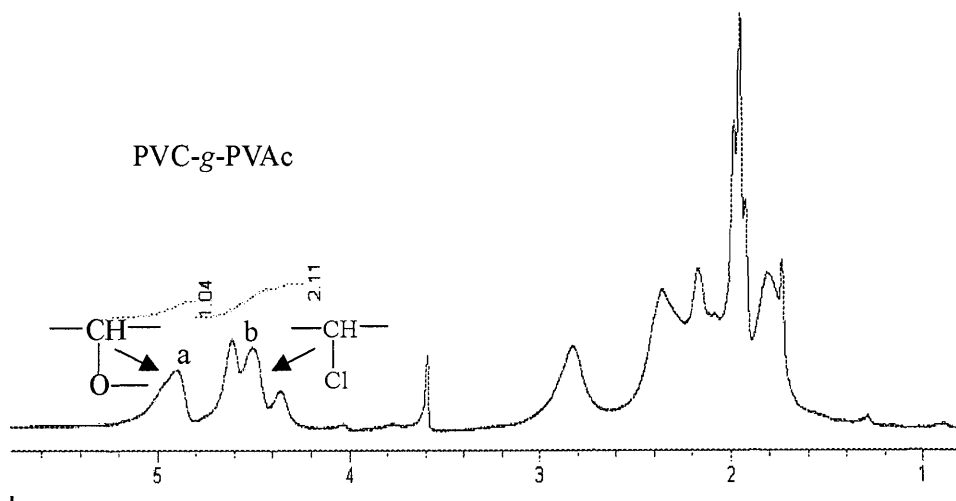**Figure 38.** ^{13}C NMR spectrum of PVAc

PVC-*g*-PVAc

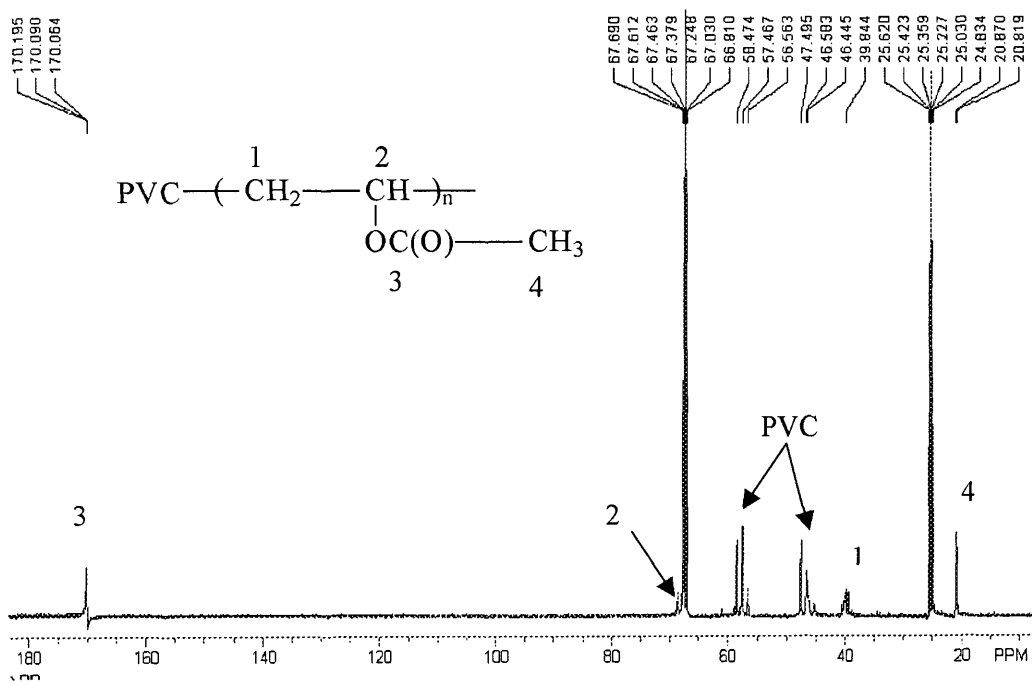**Figure 39.** ¹H NMR spectrum of PVC-*g*-PVAc
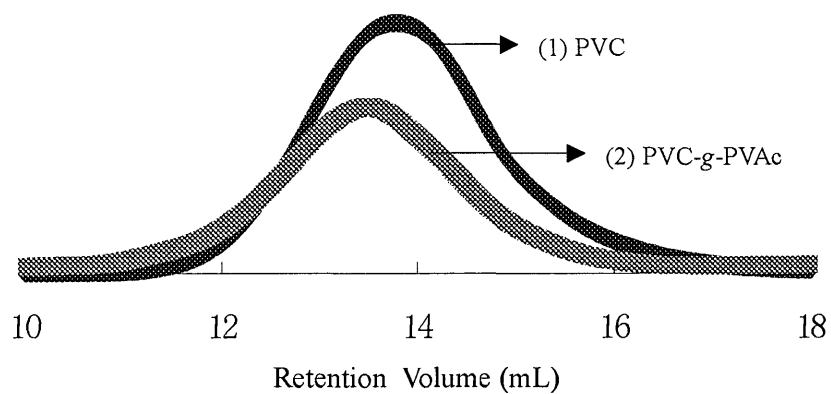

Figure 40. ¹³C NMR spectrum of PVC-*g*-PVAc

Figure 41. GPC curves for (1) PVC: M_w = 68,800, M_n = 24,800, Pd = 2.77 and

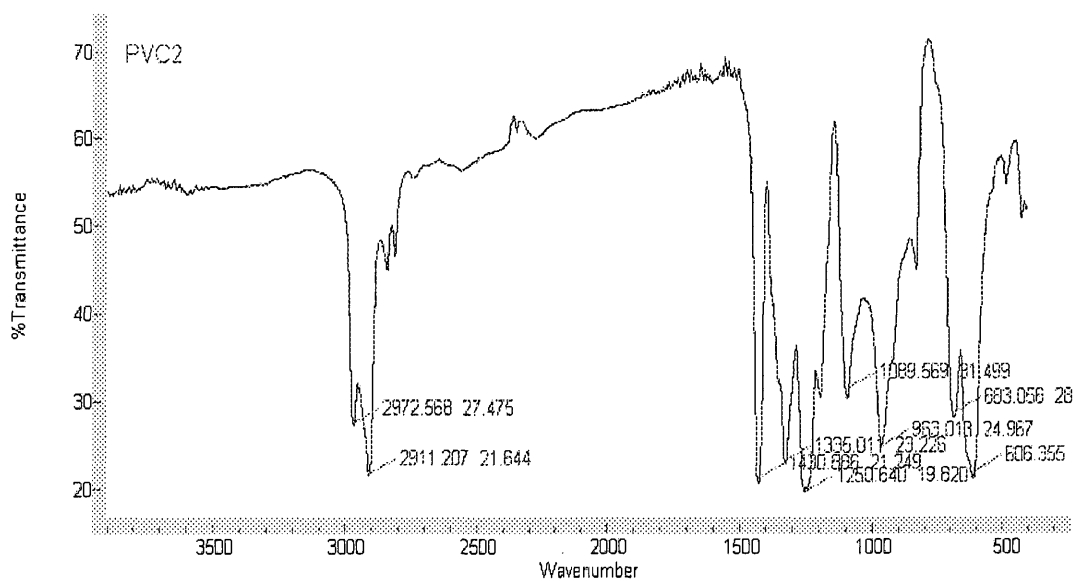(2) PVC-g-PVAc: M_w = 104,100, M_n = 44,400, Pd = 2.34
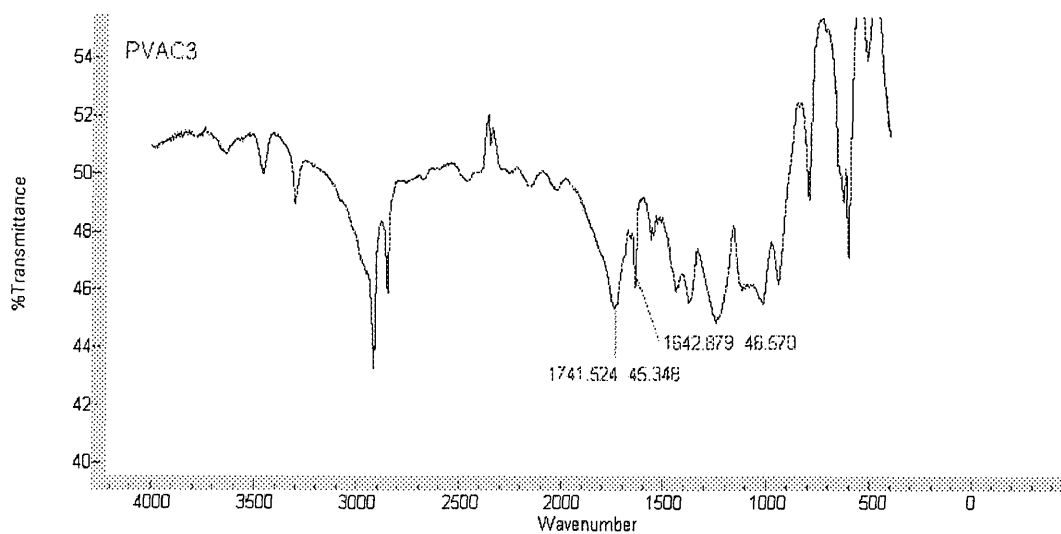

Figure 42. IR spectrum of original PVC
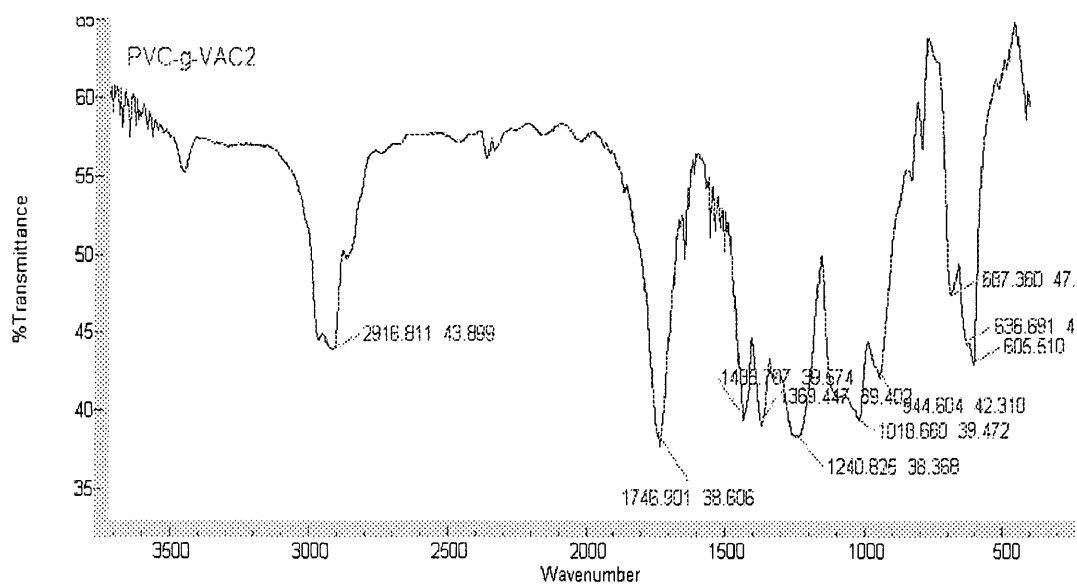
Figure 43. IR spectrum of PVAc

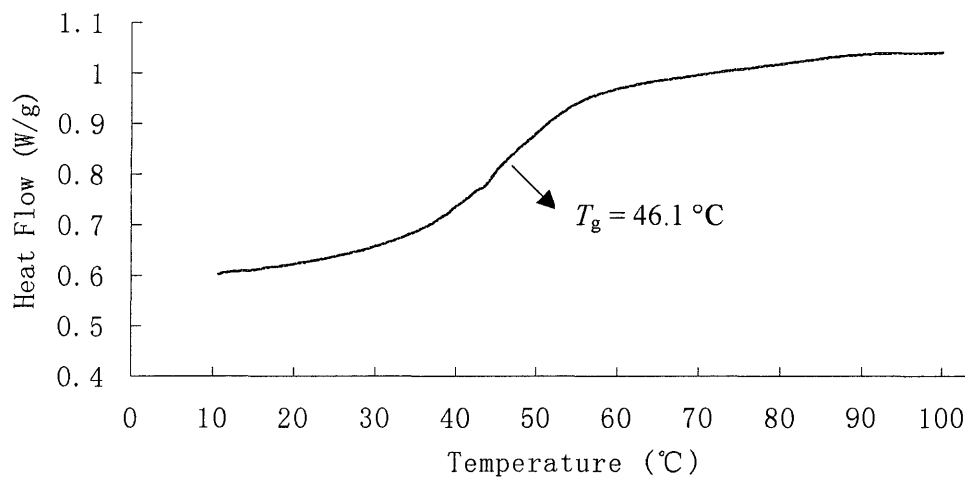**Figure 44.** IR spectrum of PVC-*g*-PVAc
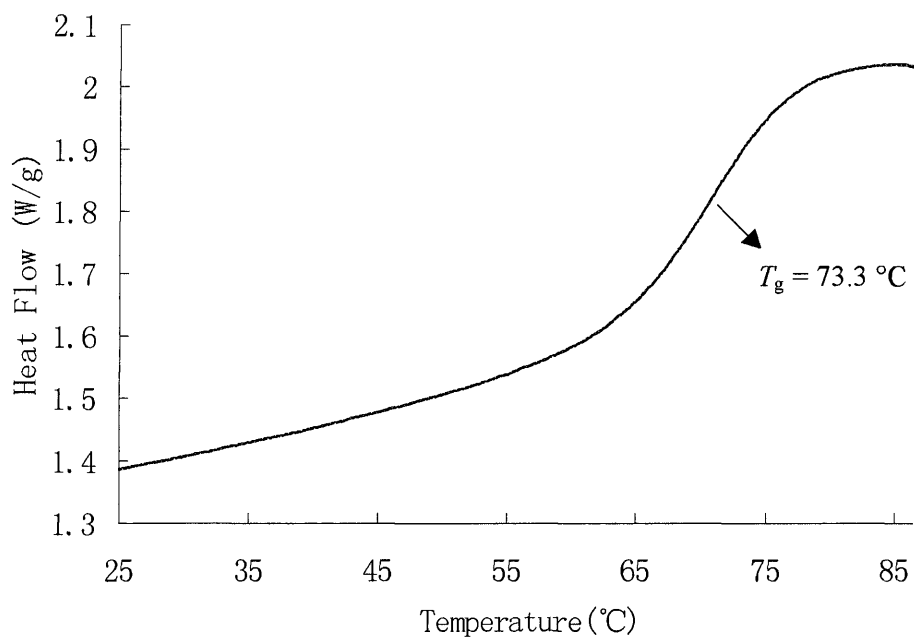
Figure 45. DSC curve of PVC-*g*-PVAc

Figure 46. DSC curve of PVC

TGA
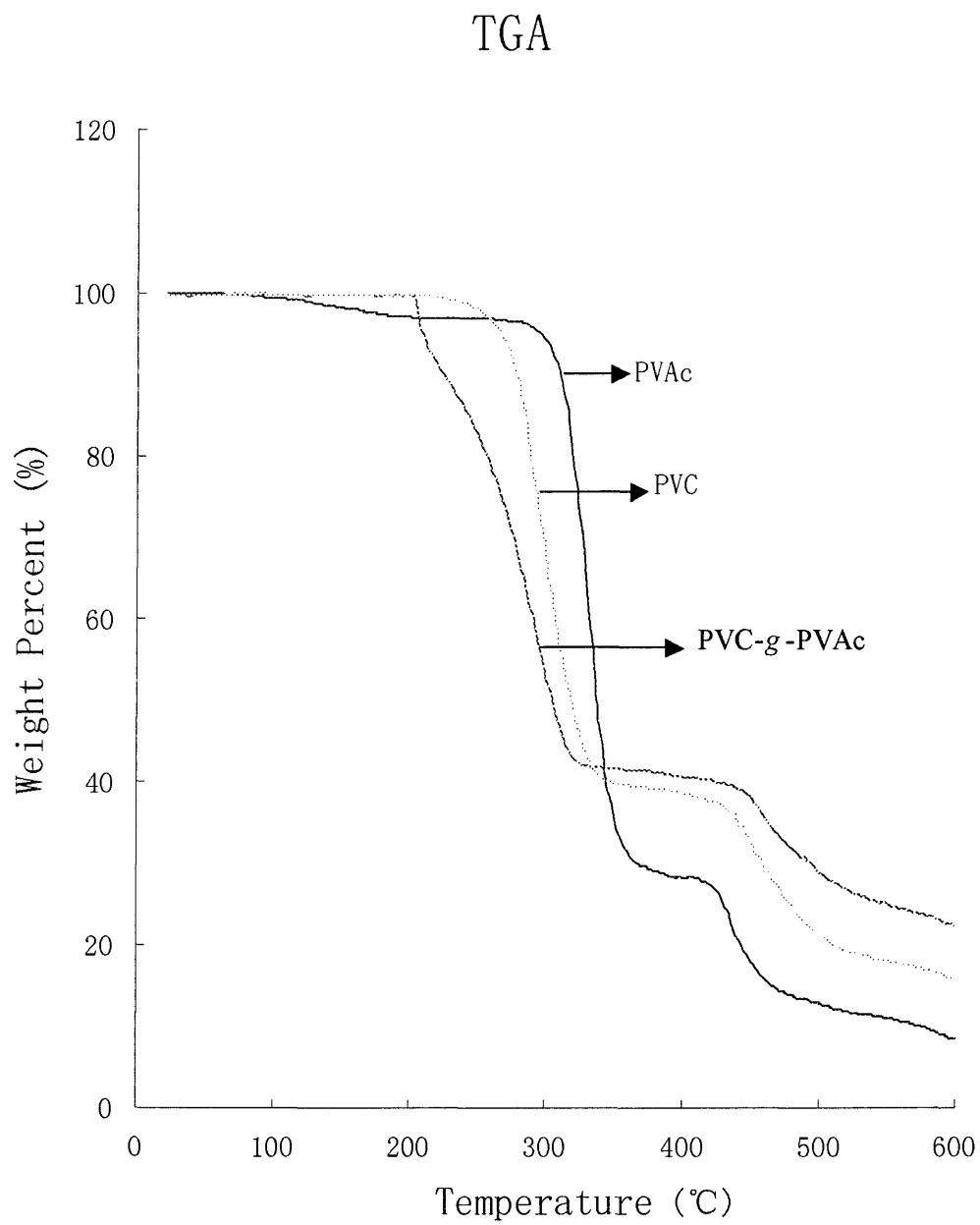
Figure 47. TGA curves of PVAc, the original PVC, and PVC-*g*-PVAc

Abundance

TIC: GDC198.D

750000
700000
650000
600000
550000
500000
450000
400000
350000
300000
250000
200000
150000
100000
50000
0

Adduct 2

5.50 6.00 6.50 7.00 7.50 8.00 8.50 9.00 9.50 10.00 10.50 11.00 11.50

Time-->

Abundance

Scan 579 (8.481 min): GDCHEN.D
179

16000

235

14000

12000

291

10000

8000

6000

121

4000

2000

41

57

135

147

0

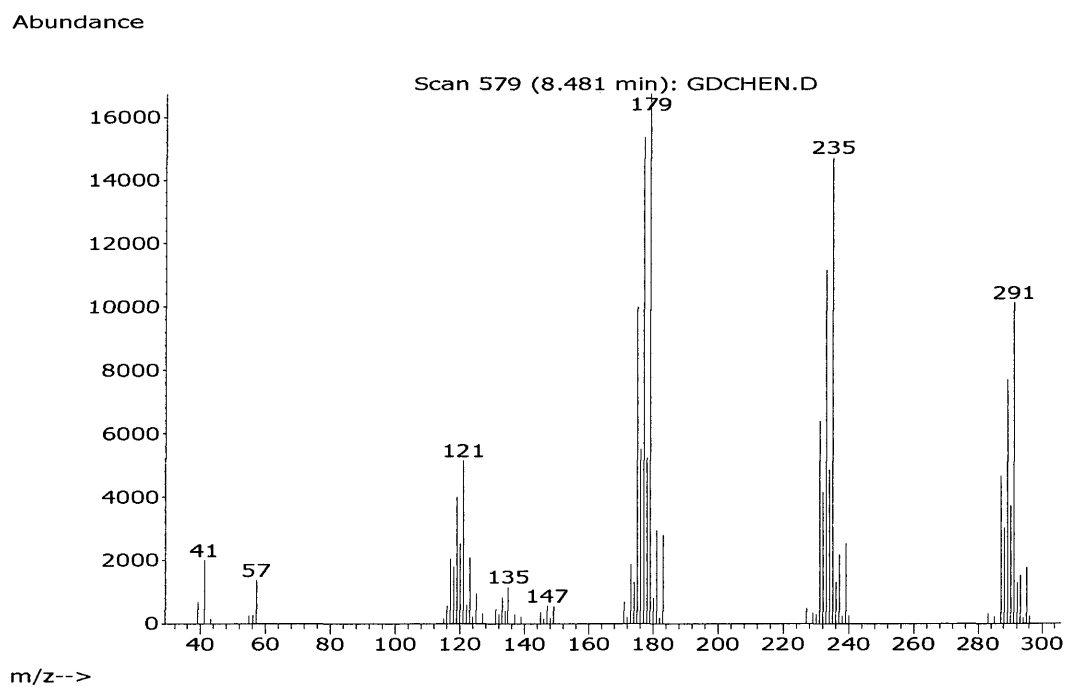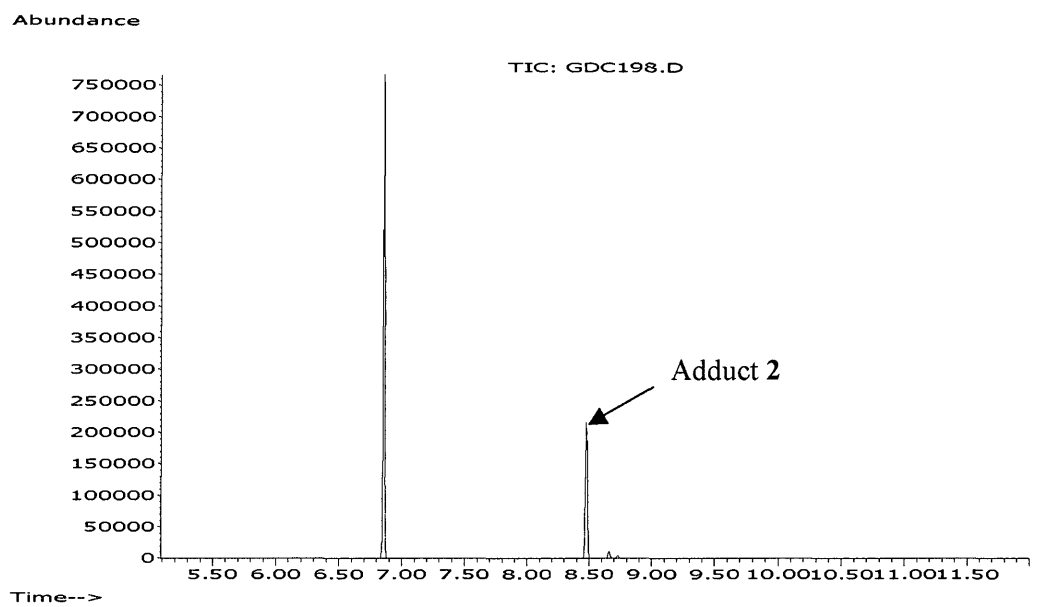40 60 80 100 120 140 160 180 200 220 240 260 280 300

m/z-->

Figure 48. GC/MS results for the reaction products from
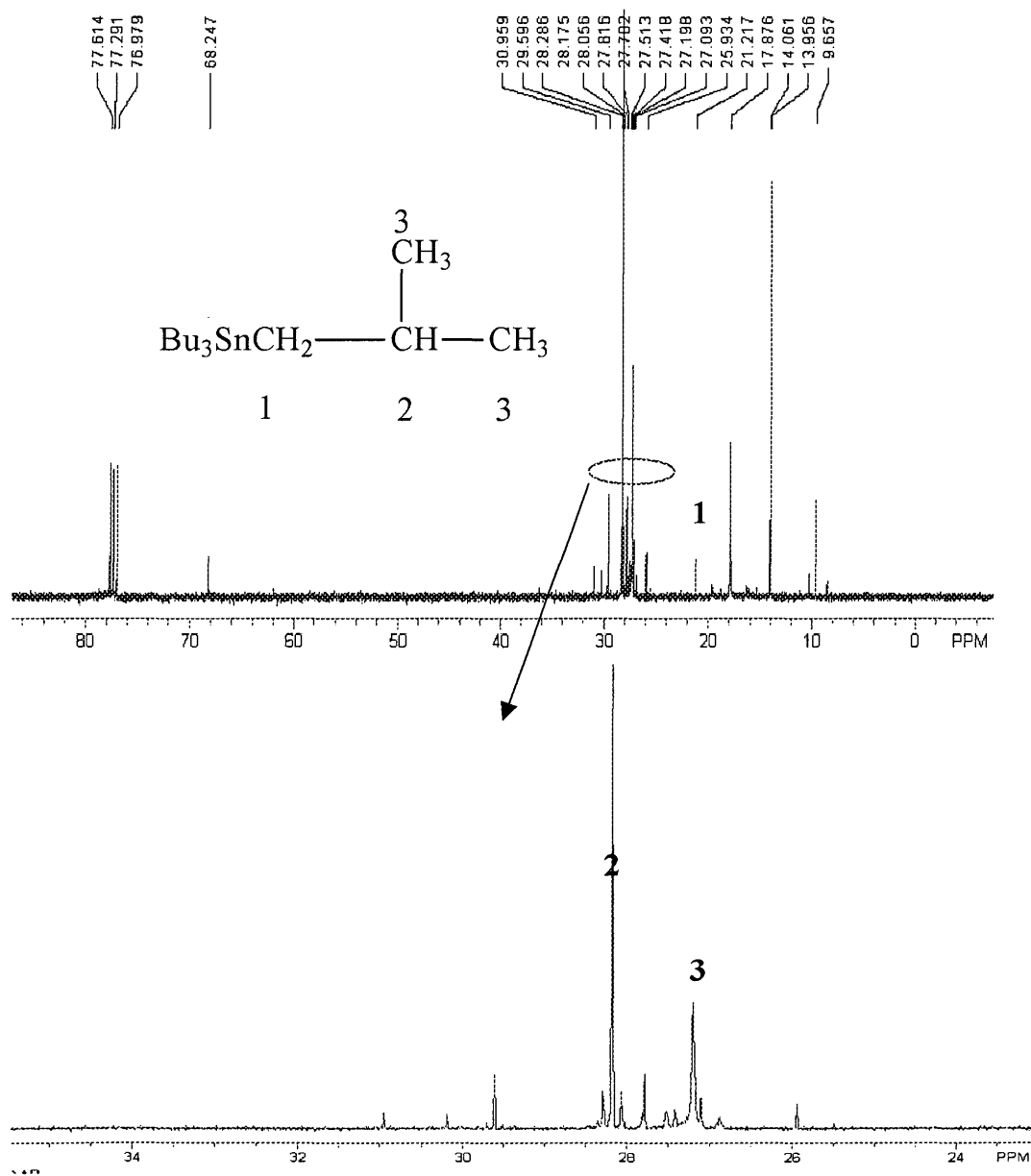
tributyltin hydride and isobutylene

Figure 49. ^{13}C NMR spectrum of reaction products from

tributyltin hydride and isobutylene

Abundance

TIC: GDC220.D

2000000
1800000
1600000
1400000
1200000
1000000
800000
600000
400000
200000
0

6.87
8.68
6.13
8.48
8.74
6.72
11.83

5.50 6.00 6.50 7.00 7.50 8.00 8.50 9.00 9.50 10.0010.5011.0011.50

Time-->

Abundance

Scan 580 (8.487 min): GDCHEN.D

16000
14000
12000
10000
8000
6000
4000
2000
0

179
235
291
121
41
57
135
149

40 60 80 100 120 140 160 180 200 220 240 260 280 300

m/z-->

Figure 50. GC/MS results for products from mole ratio = 1:1.6:6.7

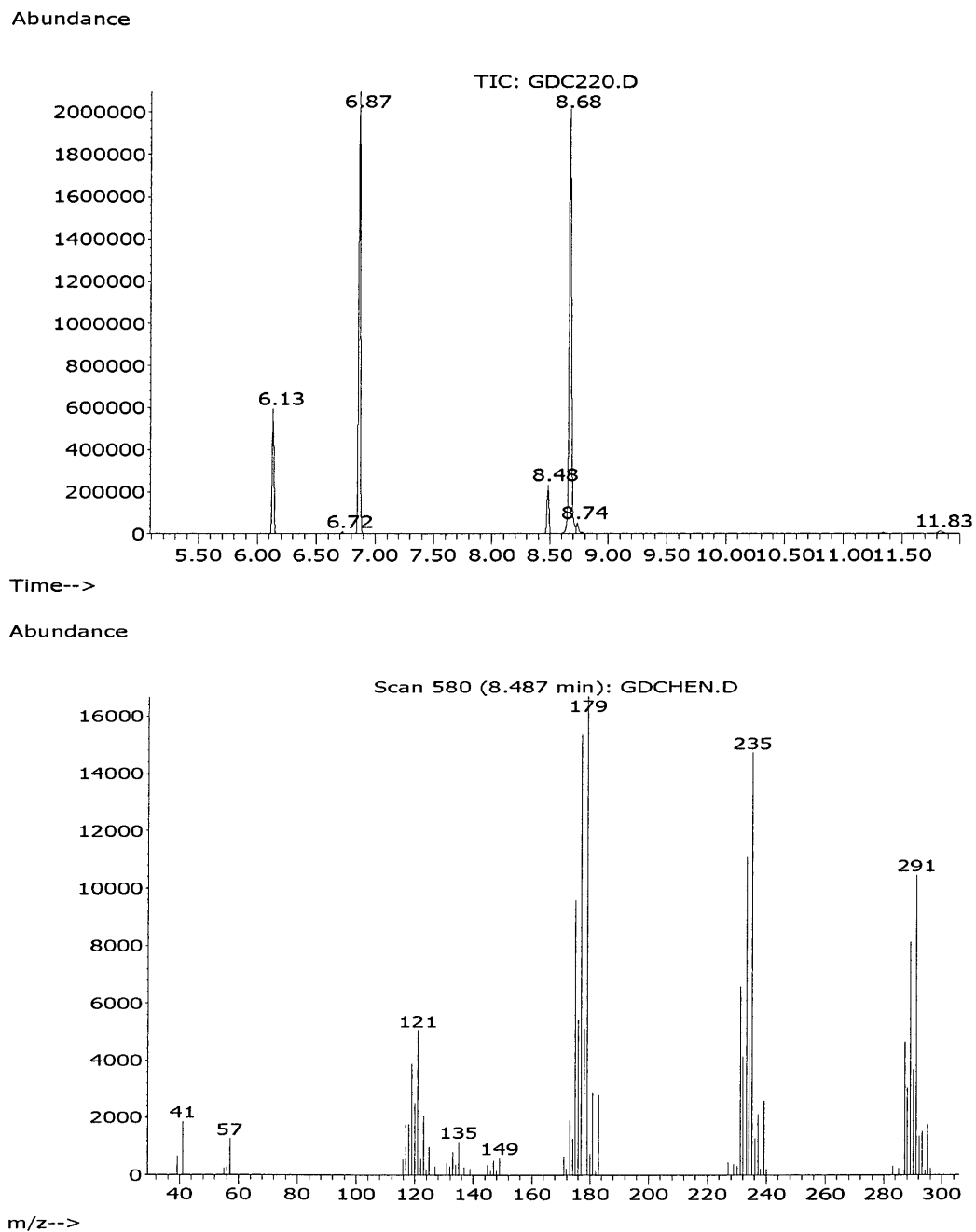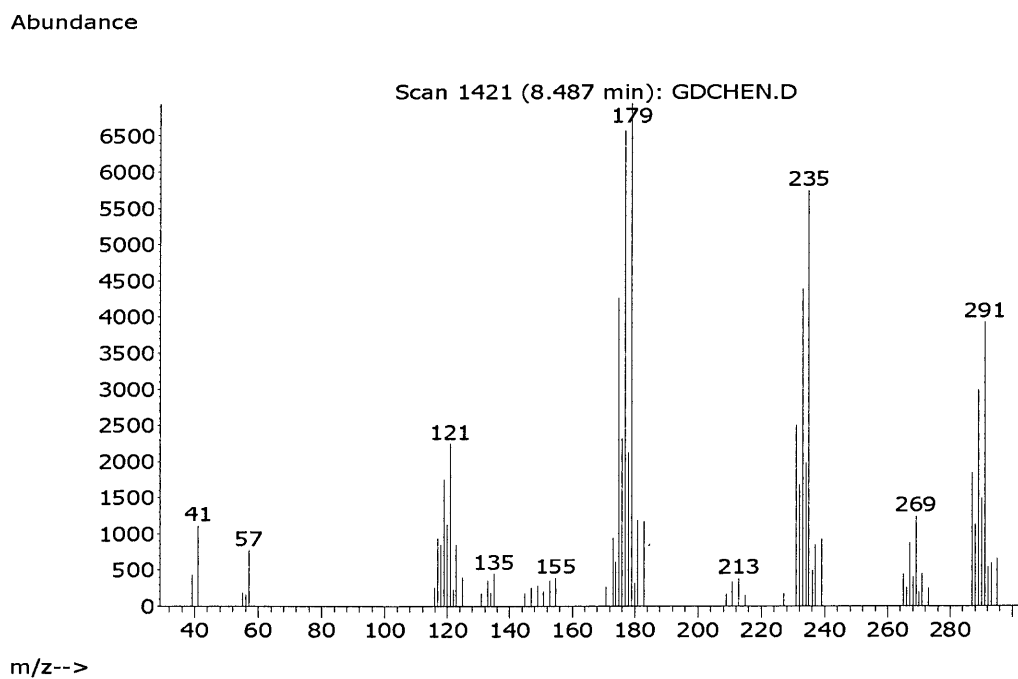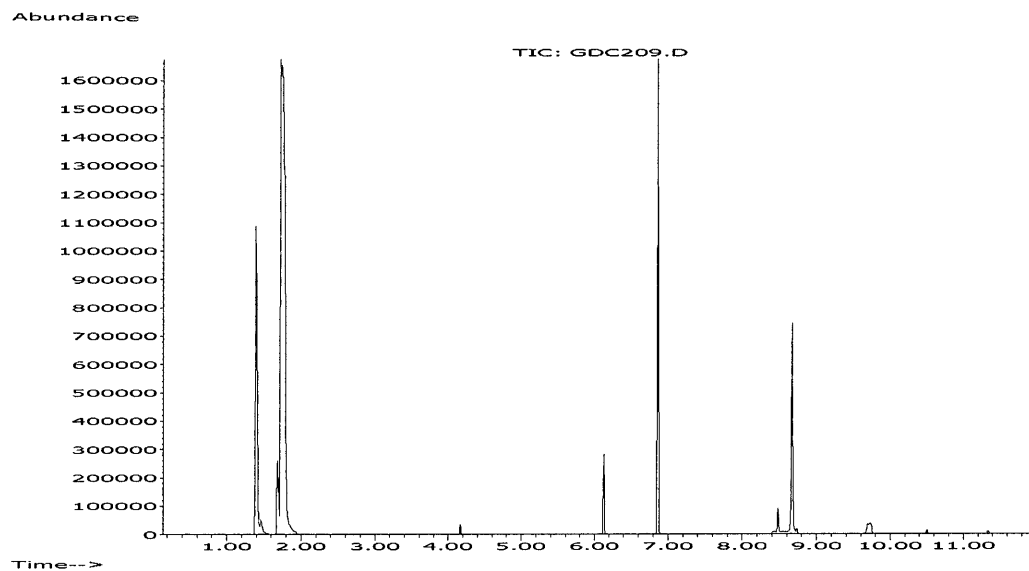**Figure 51.** GC/MS results for products from mole ratio = 1:1.1:8.4

Abundance

TIC: GDC222.D

2000000
1800000
1600000
1400000
1200000
1000000
800000
600000
400000
200000
0

6.87

8.67

6.13

6.72   8.48   8.73   11.34

5.50 6.00 6.50 7.00 7.50 8.00 8.50 9.00 9.50 10.0010.5011.0011.50

Time-->

Abundance

Scan 579 (8.481 min): GDCHEN.D

18000
16000
14000
12000
10000
8000
6000
4000
2000
0

179

235

291

121

41   57   135   149   207

40   60   80   100   120   140   160   180   200   220   240   260   280   300

m/z-->
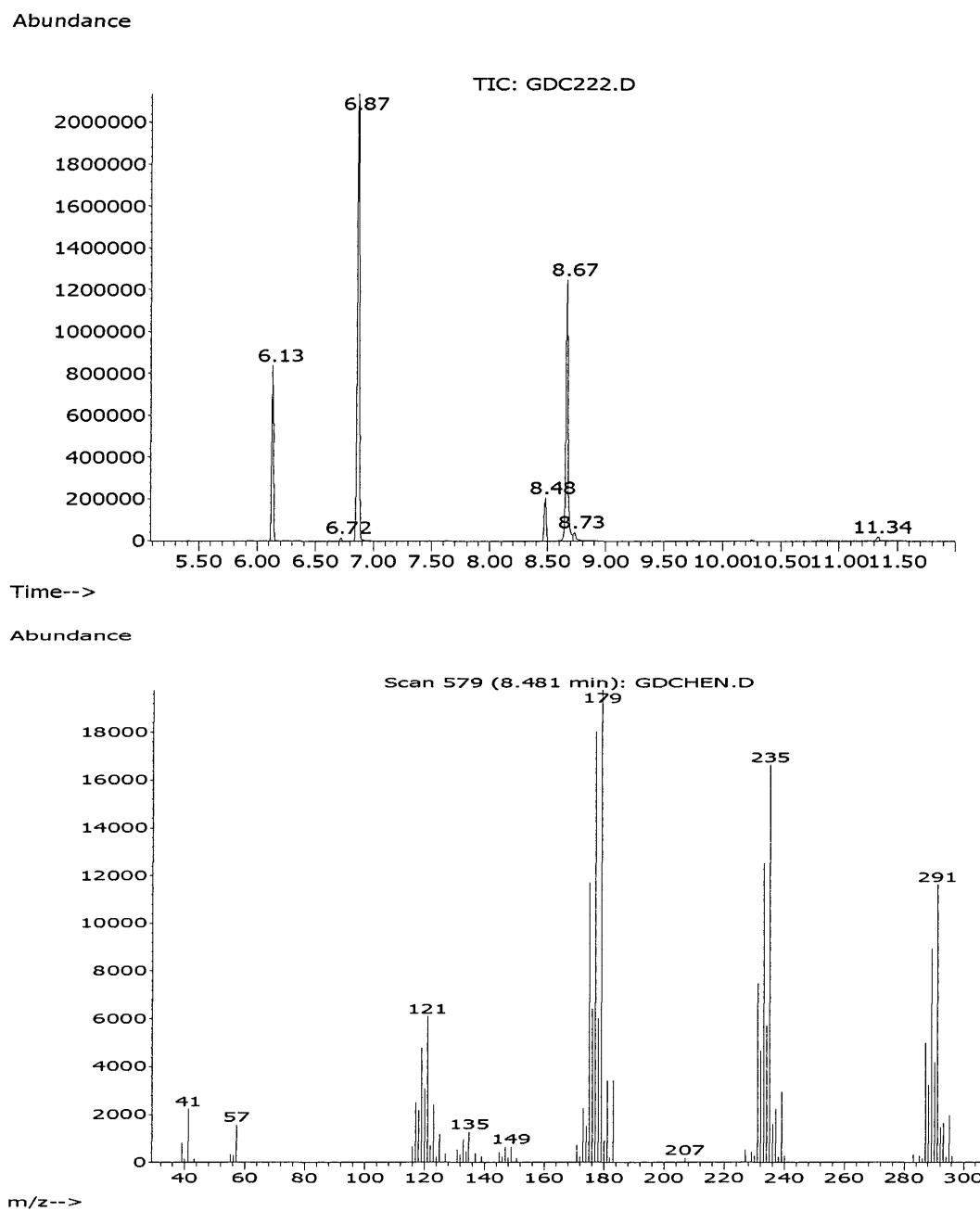
Figure 52. GC/MS results for products from mole ratio = 1:1.5:9.1

Abundance

TIC: GDC204.D

1700000
1600000
1500000
1400000
1300000
1200000
1100000
1000000
900000
800000
700000
600000
500000
400000
300000
200000
100000
0

6.86

8.67

6.13

8.48

8.73

11.34

Time-->

5.50 6.00 6.50 7.00 7.50 8.00 8.50 9.00 9.50 10.0010.5011.0011.50

Abundance

Scan 579 (8.481 min): GDCHEN.D

16000

14000

12000

10000

8000

6000

4000

2000

0

179

235

291

121

41

57

135

147

m/z-->

40   60   80   100   120   140   160   180   200   220   240   260   280   300

Figure 53. GC/MS results for products from mole ratio = 1:1.4:8.4

Abundance

TIC: GDC217.D

2000000
1800000
1600000
1400000
1200000
1000000
800000
600000
400000
200000
0

6.87

8.68

6.14

8.49

8.74

6.73

10.26   11.35

5.50 6.00 6.50 7.00 7.50 8.00 8.50 9.00 9.50 10.0010.5011.0011.50

Time-->

Abundance

Scan 581 (8.493 min): GDCHEN.D

16000
14000
12000
10000
8000
6000
4000
2000
0

179

235

291

121

41
57

135
149

40   60   80   100   120   140   160   180   200   220   240   260   280   300

m/z-->
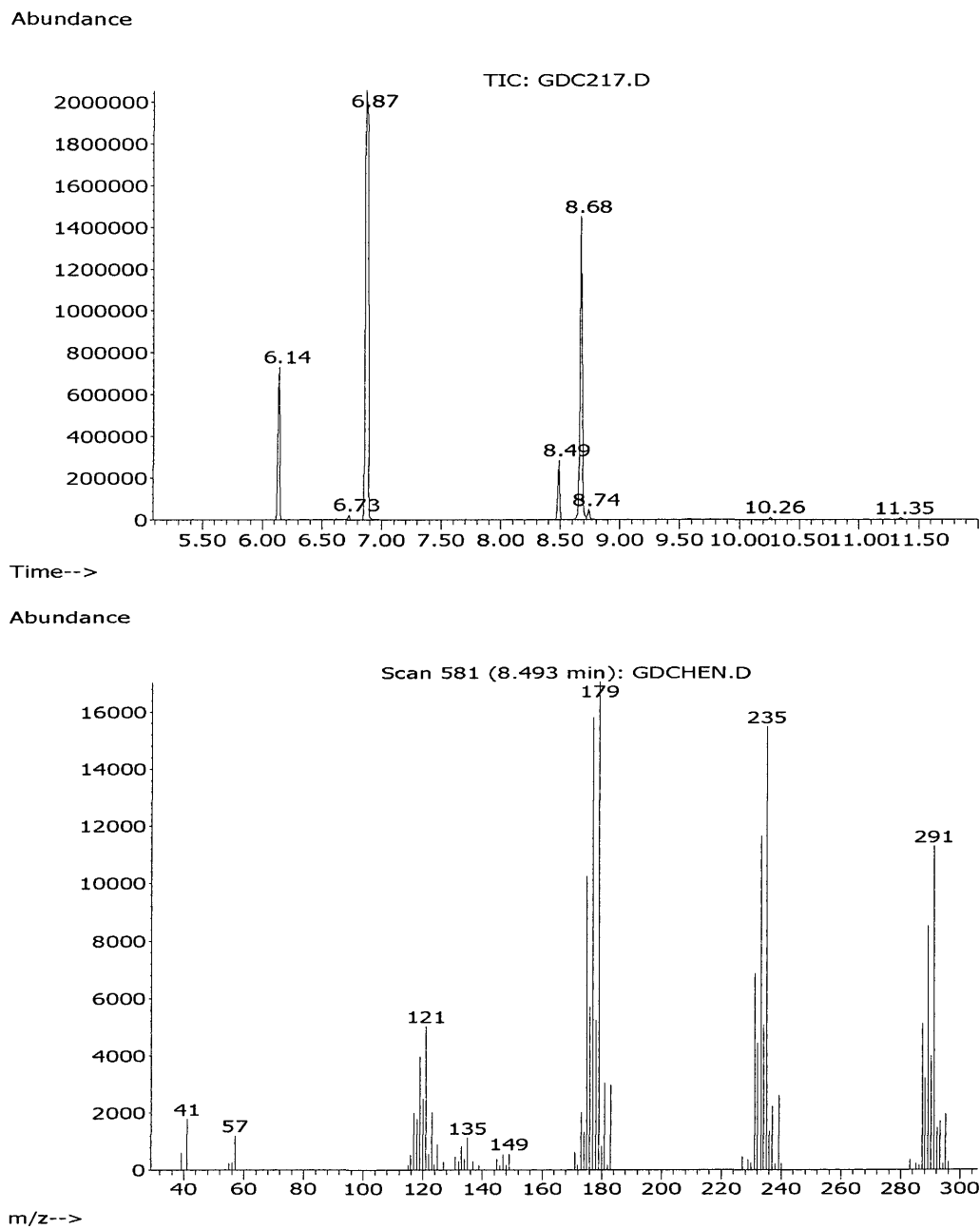
Figure 54. GC/MS results for products from mole ratio = 1:1.2:8.5

Abundance

TIC: GDC216.D

2000000
1800000
1600000
1400000
1200000
1000000
800000
600000
400000
200000
0

6.87

8.68

6.14

8.49

6.73

8.74

10.64

Time-->

5.50 6.00 6.50 7.00 7.50 8.00 8.50 9.00 9.50 10.0010.5011.0011.50

Abundance

Scan 580 (8.487 min): GDCHEN.D

36000
34000
32000
30000
28000
26000
24000
22000
20000
18000
16000
14000
12000
10000
8000
6000
4000
2000
0

179

235

291

121

41

57

73

147

163

197

341

403

m/z-->

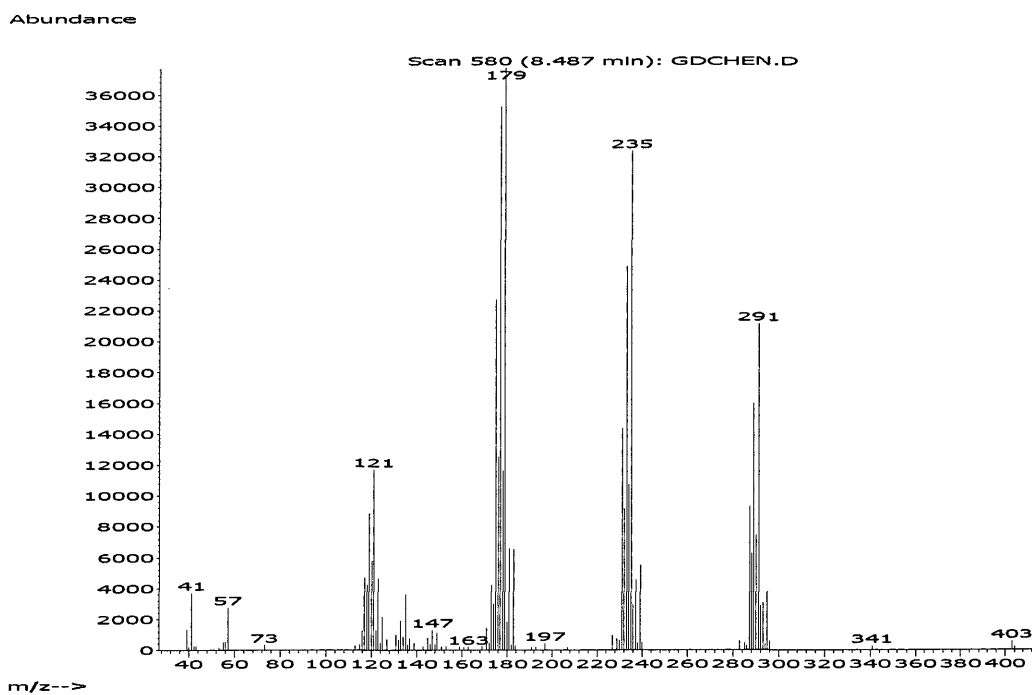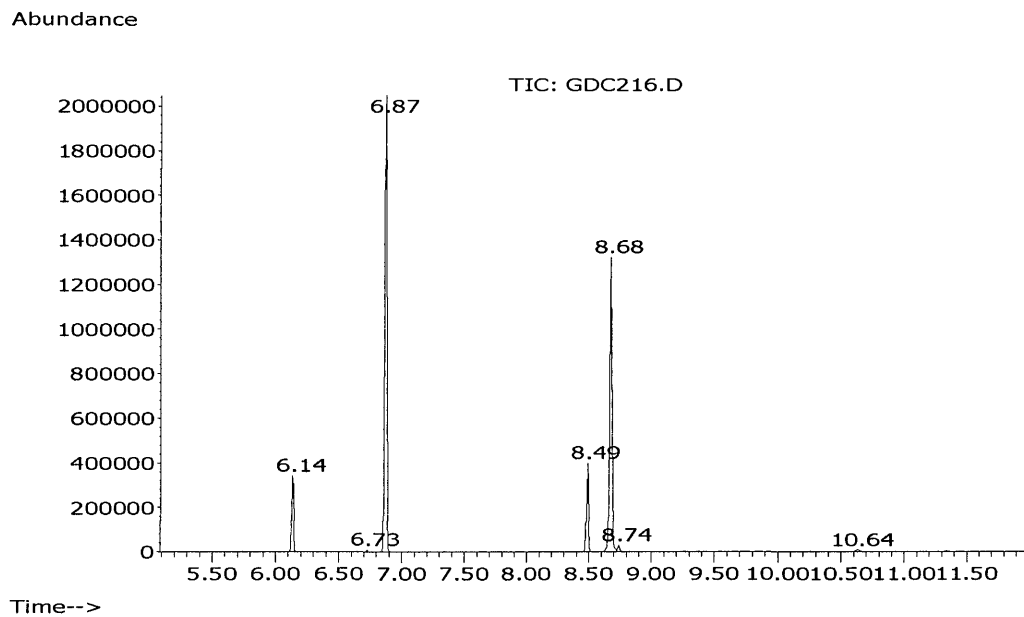40 60 80 100 120 140 160 180 200 220 240 260 280 300 320 340 360 380 400

Figure 55. GC/MS results for products from mole ratio = 1:1.4:20.2
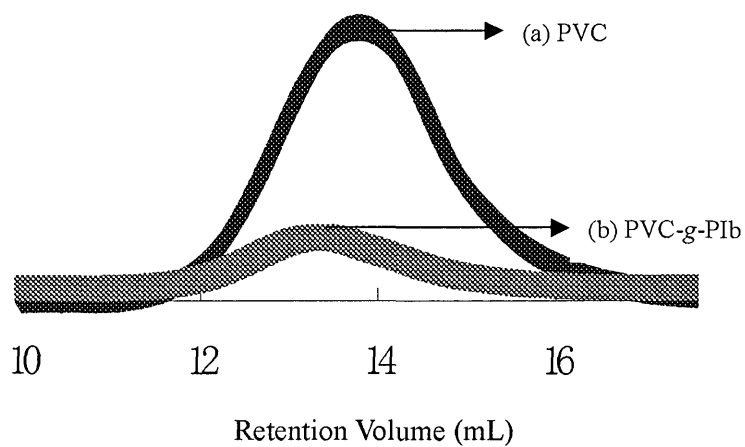
Figure 56. GPC curves of (a) PVC: M_w = 68,800, M_n = 24,800, Pd = 2.77
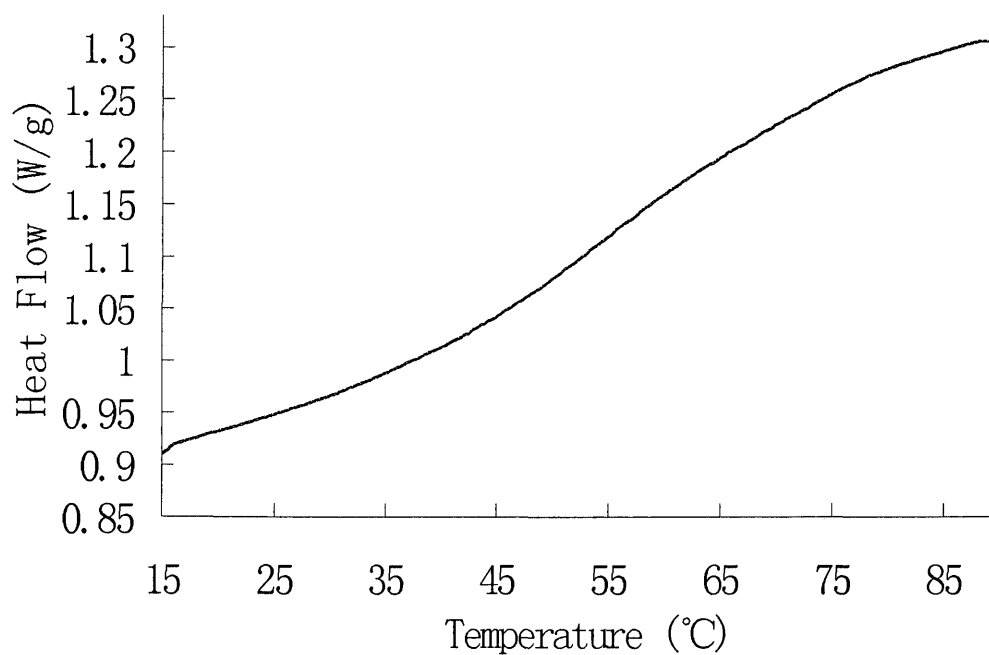and (b) PVC-g-PIb: M_w = 95,200, M_n = 41,800, Pd = 2.28
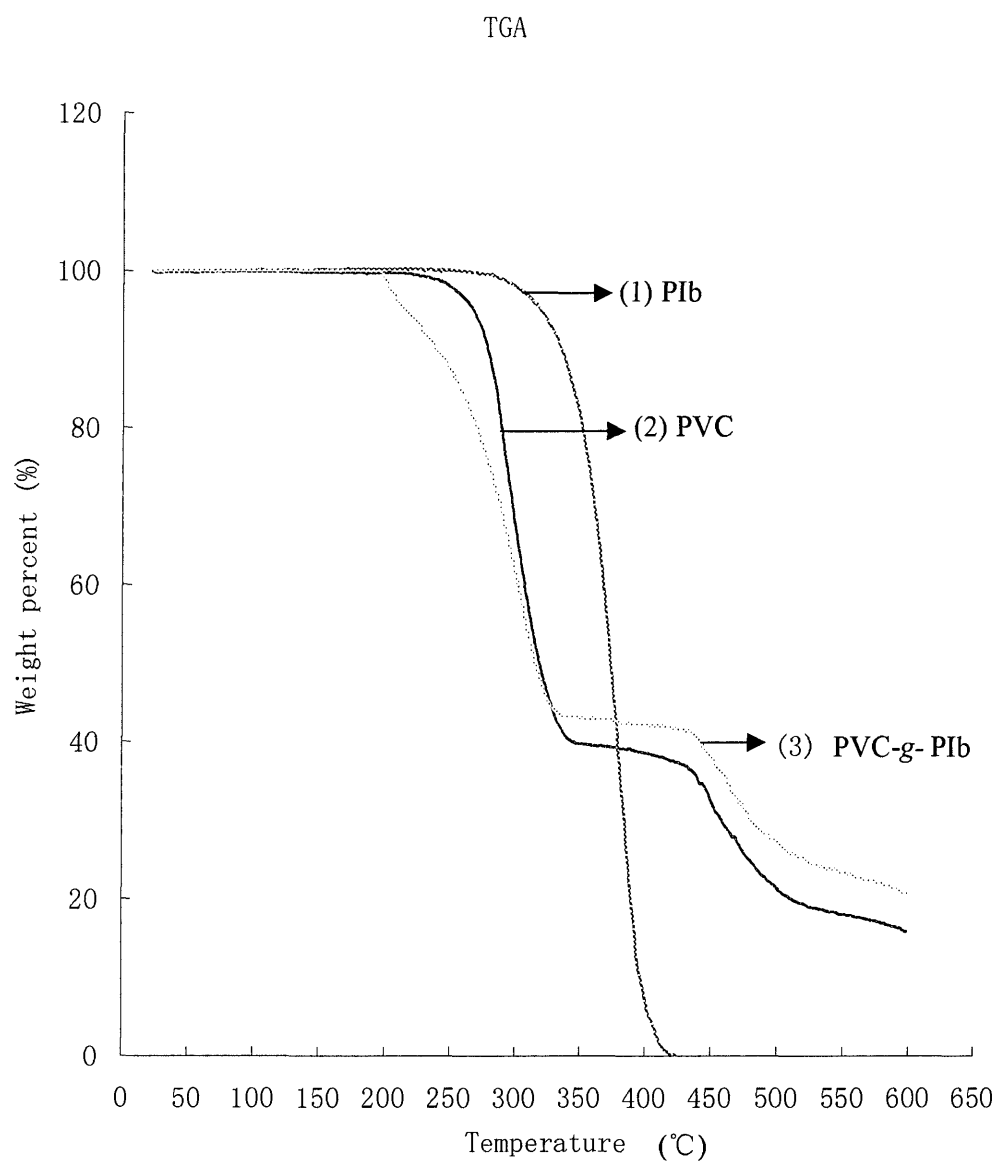

Figure 57. DSC curve of PVC-g-PIb

TGA

Figure 58. TGA curves of (1) PIb, (2) original PVC,

and (3) PVC-*g*-PIb

V. Conclusions

By using a model compound for PVC, 2-chlorobutane, the ratio k_2/k_1 was determined. For the vinyl acetate monomer, this ratio is about 3.95. However, for isobutylene, its value is ca. 62.9. These data show that monomers with electron-donor groups are the most attractive grafting candidates, owing to their slower reaction with the metal-centered free radical, $Bu_3Sn\cdot$.

Formation of the graft copolymer PVC-g-PVAc was confirmed by NMR, GPC, and FTIR data. This result demonstrated the feasibility of the new grafting method that was described in the Introduction. The thermal properties of the graft copolymer were studied by DSC and TGA. The DSC curve showed only a single T_g between the T_g of PVC and that of PVAc. The TGA results indicated that the graft copolymer was somewhat less stable than the original PVC.

In the case of the supposed graft copolymer PVC-g-PIb, a good solvent for NMR analysis could not be identified. However, the results from GPC, DSC, and TGA analyses strongly suggested that the copolymer had been formed.

References

1. Kennedy, J. P.; Davidson, D. L. **Cationic polymerization of isobutylene from poly(vinyl chloride): physical properties of poly(vinyl chloride-*g*-isobutylene).** *Applied Polymer Symposia* (1977), **30**, 51-72.

2. Feng, Y.; Zhao, J.; Wang, Q.; Li, M.; Chen, X.. **Synthesis and characterization of comb-like polymer PVC-poly(ethylene oxide).** *Journal of Applied Polymer Science* (2000), **75**, 475-479.

3. Kusy, R. P.; Whitley, J. Q.; Buck, R. P.; Cosofret, V. V.; Lindner, E. **Syntheses and kinetics of piperazine-modified poly(vinyl chloride)s for use as fixed-site proton carrier membranes.** *Polymer* (1994), **35**, 2141-2147.

4. Reinecke, H.; Lopez, D.; Mijangos, C. **New aminated PVC compounds: synthesis and characterization.** *Journal of Applied Polymer Science* (1999), **74**, 1178-1185.

5. Kennedy, J. P.; Baldwin, F. P. **Graft polymerization of halogenated polymers.** Fr. Patent 1,564,485 (1969).

6. Thame, N. G.; Lundberg, R. D.; Kennedy, J. P. **Graft modification of poly(vinyl chloride) and related reactions.** *Journal of Polymer Science, Polymer Chemistry Edition* (1972), **10**, 2507-2525.

7. Ravve, A.; Khamis, J. T. **Grafting glycidyl methacrylate on poly(vinyl chloride) backbones.** *Journal of Polymer Science* (1962), **61**, 185-194.

8. Gallot, Y.; Rempp, P.; Parrod, J. **Anionic grafting reactions.** *Journal of Polymer Science, Part B1* (1963), **1**, 329-335.

9. Trivedi, P. D.; Ambrose, R. J.; Altenau, A. G. **Synthesis and characterization of poly(vinyl chloride-α-methylstyrene) - a new thermoplastic resin. 2.** *Journal of Macromolecular Science, Chemistry* (1982), **17**, 1159-1168.

10. Percec, V.; Asgarzadeh, F.. **Metal-catalyzed living radical graft copolymerization of olefins initiated from the structural defects of poly(vinyl chloride).** *Journal of Polymer Science, Part A: Polymer Chemistry* (2001), **39**, 1120-1135.

11. **PVC Blends, Blocks, Grafts, and Interpenetrating Polymer Networks.** Manson, J. A. In *Encyclopedia of PVC, 2nd ed.*; Nass, L. I.; Heiberger, C.A., Eds.; Marcel Dekker: New York, 1986; Chapter 10.

12. Breitmaier, E.; Voelter, W.; *Carbon-13 NMR Spectroscopy, 3rd ed.*; VCH publishers: New York, 1990.

VITA

Guangde Chen

Guangde Chen was born in Guangxi, P. R. China, on November 1, 1981. He received his Bachelor of Science degree in the Department of Polymer Science and Engineering from the University of Science and Technology of China (USTC), Hefei, in July 2003. Subsequently, he became a graduate student in the Department of Chemistry at the College of William and Mary.